Conception of topological analogue of the magnetic bit

by

Xinyuan Xu

Master's thesis submitted to

Faculté des Sciences, Université de Sherbrooke
Sherbrooke, Québec, Canada

Le *** 2022

le jury a accepté le mémoire de Monsieur Xinyuan Xu dans sa version finale.

Membres du jury

P^{r} Ion Garate
Co-directeur de recherche
Département de physique

P^{r} David Sénéchal
Co-directeur de recherche
Département de physique

P^{r} Alexandre Blais
membre interne
Département de physique

P^{r} René Côté
Président rapporteur
Département de physique

Contents

List of Figures

Chapter 1

Introduction

1.1 Topological phases

Over the last 15 years there is a "party" of topological phases held by condensed matter physicists, since the successful formulation and prediction of the topological insulator [21, 22, 12, 5], numerous papers related to topological phases have been published.

Topological phases is a branch of exotic phases of matter protected by the symmetries of the system [30], and they can be described by the abelian or non-abelian berry phase of the wave function [6]. The topological phase can be trivial or non-trivial depending on the parameter, and it is characterized by an integer, which is know as the topological invariant. Generally, the system has an edge state on its boundary with the system has non-trivial topological invariant, this is because the bulk of the system is fully gaped but not its edge. This edge state is normally robust, in the sense that the edge state will not be destroyed by perturbations which preserves the symmetry, one example is the quantum spin hall effect [22]. Microscopically, non-trivial topological phase means the Wannier center of the system advancing interger numbers of unit cells, trivial topological phase means the Wannier center does not move [10].

There is a simple but deep question to ask: how to change the topological invariant of the system? One of the general mechanism is so called "Band inversion" [27]. In the language of band theory, in order to change the topology of the system one need to close the energy gap first, then re-open the energy gap with a different value parameter (normally by changing its sign), by the time the gap opens again, a small fraction of the valence band goes to the conduction band, and a small fraction of the conduction band goes to the valence band, as a consequence the boundary of the system has metallic state and the bulk is insulating.

The band inversion mechanism is a quite general statement, it does not tell us the dynamics of order parameter during this process, which will be the main focus of this thesis.

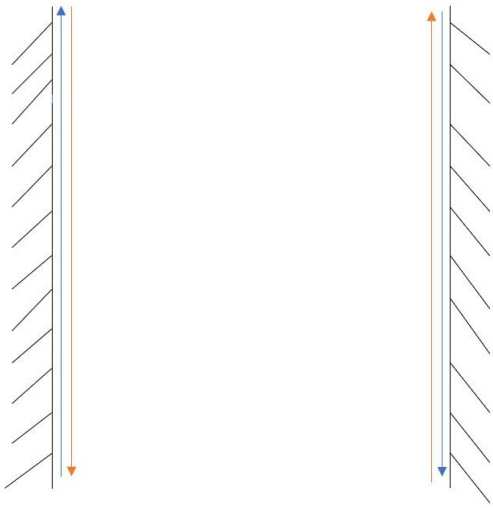

Figure 1.1
Edge state of the 2D topological insulator-quantum spin hall, the current in blue is carried by electrons with "up "spin and the current in orange is carried by electrons with "down" spin. and the edge state is protect by Z_2 invariant.

1.2 Floquet engineering

One way to change the topological invariant of the system is through the Floquet engineering, by which means changing the band structure by external perturbations and induce the band inversion, experimentally this could be achieved by couple the system with polarized light [29].

In Floquet engineering, the Hamiltonian of the system is periodic in time T: $H(t) = H(t+T)$. Generally the topological invariant is computed by using the bloch state $|u_{kn}(\mathbf{r})\rangle$ [10], which is a static complete orthogonal set of solutions for the time-independent Schrodinger equation. As an example in 1D the topological invariant of the system is given by [10]

$$n = \frac{1}{2\pi}\oint dk \langle u_{kn}|i\partial_k|u_{kn}\rangle, \tag{1.1}$$

However, in Floquet engineering we use a time-dependent basis $|\Phi(t)\rangle$, since $\exp(-i\tilde{\epsilon}t)|\Phi(t)\rangle$ forms a complete orthogonal set of solutions for the time-dependent Schrodinger equation, $\tilde{\epsilon}$ is the generalized energy and $|\Phi(t)\rangle = |\Phi(t+T)\rangle$. The one-period time evolution operator can be defined as $U(T,k) = \exp\left(-i\int_0^T dt' H(t',k)\right)$, so the generalized energy can be determined by $U(t)|\Phi(0)\rangle = \exp(-i\tilde{\epsilon}t))|\Phi(0)\rangle$. $U(T)$ can be simplified by finding an effective time-independent Hamiltonian $H_{\text{eff}}(k)$ of the time-dependent Hamiltonian $H(t,k)$, then as an example the topological invariant for the 1D Floquet system is given

by [29]

$$n = \frac{1}{2\pi} \oint dk \, \mathrm{Tr}[U(k,T)^{\dagger} i \partial_k U(k,T)], \tag{1.2}$$

which is different from the topological invariant computed from the bloch state.

1.3 Landau-Lifshitz-Gilbert equation and its topological analogue

In the Floquet engineering, although the topology of the system changes, however it goes back to its original value when the perturbation is turned off. Then main question we will address in this thesis is that, is it possible to go beyond the Floquet engineering? In the sense that is it possible to change the topological invariant by external perturbations, then turn off the perturbation but have the topological invariant remains in the new value?

Let us now think about the classical magnetism. In magnetic memory, a pair of the mean-field level magnetization with opposite orientation forms a "magnetic bit". It is well-known that in such case the magnetization can be reversed by external perturbations and remains in the new value, the dynamics of such process is described by the Landau-Lifshitz-Gilbert equation [2]:

$$\frac{d\mathbf{M}}{dt} = -\gamma \mathbf{M} \times \mathbf{B}_{eff} - \lambda \mathbf{M} \times (\mathbf{M} \times \mathbf{B}_{eff}), \tag{1.3}$$

and

$$\mathbf{B}_{\text{eff}} = \mathbf{B}_{\text{ext}} + \mathbf{B}_{\text{ani}}, \tag{1.4}$$

where $\mathbf{M}$ is the magnetism of the system at mean-field level, $\mathbf{B}_{\text{eff}}$ is the effective perturbation. $\mathbf{B}_{\text{ext}}$ is the external perturbation and $\mathbf{B}_{\text{ani}}$ is the anisotropy field. The fist term in the right hand side describes the precession of the magnetism around the effective perturbation, the second term in the right hand side describes the damping of the magnetism that pulls it to the mean-field value. γ is the constant associated with the precession and λ is the constant associated with the damping.

We map the order parameter to the magnetism and derive a topological analogue equation of the Landau-Lifshitz-Gilbert equation, which describes how the order parameter changes under external perturbation. When the external perturbation is turned off, the topological invariant of the system remains in the new value. This is a example of beyond the Floquet engineering.

Chapter 2

SSH-Holstein model

In this chapter, we present and explain the SSH-Holstein model. We begin by reviewing the SSH and Holstein models separately, and by describing the band topology in each case. The SSH-Holstein model is then constructed. This model will be used in later chapters for a proof-of-principle realization of the topological bit.

2.1 The SSH model

In its simplest realization, the SSH model describes spinless electrons moving in one dimension with a hopping amplitude modulated by phonons. Its Hamiltonian is given by [31]

$$H_{\mathrm{SSH}} = t_0 \sum_j (c_j^\dagger c_{j+1} + h.c.) - \alpha_S \sum_j (q_j - q_{j+1})(c_j^\dagger c_{j+1} + H.c.) + \frac{1}{2} m_S \sum_j \Big[(\dot{q}_j - \dot{q}_{j+1})^2 + \omega_S^2 (q_j - q_{j+1})^2 \Big], \tag{2.1}$$

where t_0 is the hopping between nearest sites, q_j is the lattice displacement at site j and α_S is the SSH electron-phonon coupling constant. We assume t_0 is real. At half-filling (one electron per two sites), the system undergoes a Peierls instability towards a gapped bond density wave [23]. In the mean-field approximation, the density wave is described by $q_j = (-1)^j \Delta_{0x}/2$, where Δ_{0x} is a static order parameter. When substituting this order parameter in Eq. (2.1), the hopping amplitude becomes dimerized, so

$$H_{\mathrm{SSH,MF}} = t_0 \sum_j (c_j^\dagger c_{j+1} + H.c.) - \alpha_S \Delta_{0x} \sum_j (-1)^j (c_j^\dagger c_{j+1} + h.c.) + \frac{1}{2} m_S \omega_S^2 \sum_j \Delta_{0x}^2. \tag{2.2}$$

A geometric presentation of the SSH model is given in Fig. (2.1). In pseudospin representation, the bond density wave can be mapped onto an antiferromagnetic state.

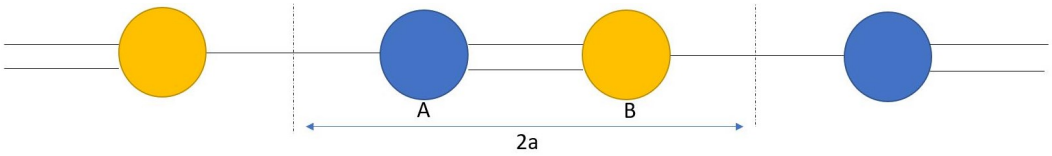

Figure 2.1
Schematic representation of the mean-field ground state of the SSH model. The hopping amplitude is modulated between weak and strong values (single and double lines, respectively). As a result the system has a two-atom unit cell. The two sites in the unit cell are denoted as A and B sites (in blue and yellow, respectively).

To see this we define the pseudospin operators

$$\begin{aligned} S_j^z &= c_j^\dagger c_j - c_{j+1}^\dagger c_{j+1} \\ S_j^x &= c_j^\dagger c_{j+1} + c_{j+1}^\dagger c_j \\ S_j^y &= -ic_j^\dagger c_{j+1} + ic_{j+1}^\dagger c_j. \end{aligned} \tag{2.3}$$

Then, $\langle S_{j+1}^x \rangle \propto (-1)^{j+1}\alpha_S \Delta_{0x}$, and Δ_{0x} can be understood as a Néel order along x. The mapping between the bond density wave order parameter and the magnetic order parameter motivates our later approach of borrowing from the concepts of spintronics in order to determine the dynamics of the density-wave order parameter.

Adopting periodic boundary conditions, Eq. (2.2) can be written in Fourier space as

$$H_{\text{SSH,MF}} = \sum_{k_1} \begin{bmatrix} C_{k_1 A}^\dagger & C_{k_1 B}^\dagger \end{bmatrix} \mathbf{d}_{k_1} \cdot \boldsymbol{\sigma} \begin{bmatrix} C_{k_1 A} \\ C_{k_1 B} \end{bmatrix} + \frac{N}{2} K_S \Delta_{0x}^2, \tag{2.4}$$

we will use k_1 for wavenumber and k_0 for frequency. A and B denote the two sites in a unit cell, N is the number of sites, $K_S = m_S \omega_S^2$ is the phonon stiffness. $C_{k_1,A}^\dagger$ and $C_{k_1,B}^\dagger$ are the electronic creation operator of A and B sites respectively; $C_{k_1,A}$ and $C_{k_1,B}$ are the electronic annihilation operator of A and B sites respectively. Vector d is

$$\begin{aligned} d_x &= (t_0 + \alpha_S \Delta_{0x}) + (t_0 - \alpha_S \Delta_{0x}) \cos(2k_1 a) \\ d_y &= -(t_0 - \alpha_S \Delta_{0x}) \sin(2k_1 a) \\ d_z &= 0, \end{aligned} \tag{2.5}$$

and a is the lattice constant. The dispersion relation of the electrons is then

$$\epsilon_{k_1 \pm} = \pm \sqrt{2(t_0^2 + \alpha_S^2 \Delta_{0x}^2) + 2(t_0^2 - \alpha_S^2 \Delta_{0x}^2) \cos(2k_1 a)}, \tag{2.6}$$

and its spectrum is shown in Fig. (2.2). We expand the energy around the vicinity of

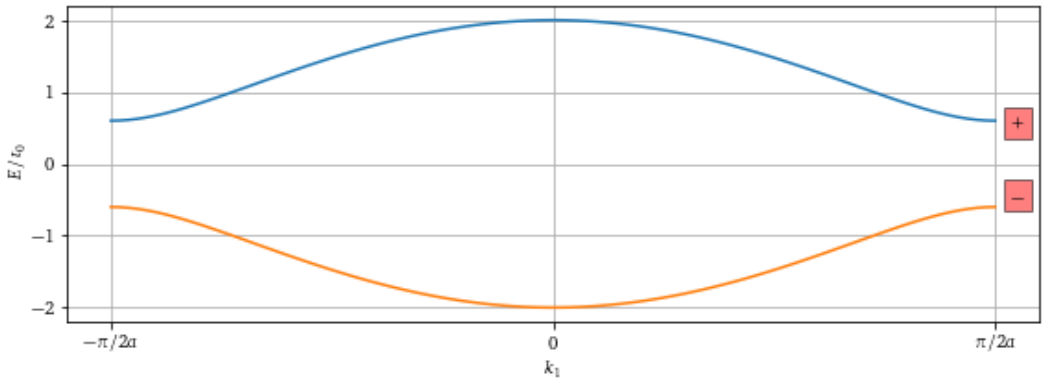

Figure 2.2
Energy spectrum of the SSH model, where "+" labels the conduction band, and "−" labels the valence band. We choose $a = 1$ and $\alpha_S \Delta_{0x}/t_0 = 0.3$.

the two Fermi points $k_1 = \frac{\pi}{2a} + q_1$, so the ground state energy of the system is

$$\begin{aligned} E[\Delta_{0x}] &\approx -\sum_{q_1} \sqrt{4a^2 t_0^2 q_1^2 + 4\alpha_S^2 \Delta_{0x}^2} + \frac{N}{2} K_S \Delta_{0x}^2 \\ &= -\frac{Na}{2\pi} \int dq_1 \sqrt{4a^2 t_0^2 q_1^2 + 4\alpha_S^2 \Delta_{0x}^2} + \frac{N}{2} K_S \Delta_{0x}^2 \end{aligned} \tag{2.7}$$

the mean-field energy and order parameters are obtained by minimizing the energy, i.e, imposing $\partial E/\partial \Delta_{0x} = 0$. By doing this we get

$$\Delta_{0x} = \pm \frac{2a t_0 \Lambda}{\alpha_S} \exp - \frac{\pi t_0 K_S}{2\alpha_S^2}, \tag{2.8}$$

where Λ is a momentum cutoff. Even though this value of Δ_{0x} minimizes the energy, $\Delta_{0x} = 0$ is also a solution but corresponds to a higher energy state in one dimension. At the mean field level there are only two possible values of Δ_{0x} and they only differ by a sign. This is an example of commensurate charge density wave (coomensurate CDW).

The eigenvectors of the conduction band "+" and valence band "−" are

$$|+, k_1\rangle = \begin{bmatrix} \cos\frac{\theta}{2} \\ e^{i\varphi} \sin\frac{\theta}{2} \end{bmatrix} \qquad |-, k_1\rangle = \begin{bmatrix} -\sin\frac{\theta}{2} \\ e^{i\varphi} \cos\frac{\theta}{2} \end{bmatrix}, \tag{2.9}$$

where $\theta = \arccos(d_z/\sqrt{d_x^2 + d_y^2 + d_z^2})$ and $\varphi = \arctan(d_y/d_x)$. In SSH model $\theta = \pi/2$ because $d_z = 0$.

It is clear that the energy spectrum is invariant under a sign change of Δ_{0x}. However the sign of Δ_{0x} has impact on the band topology of the system. To see this, let us calculate the Berry phase for the SSH Hamiltonian in the mean-field approximation. The Berry phase is a geometric phase that appears in quantum mechanical system. It

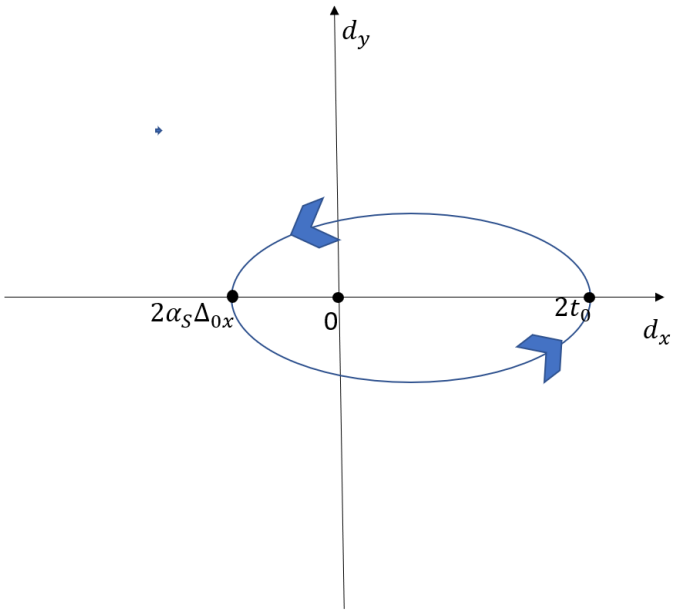

Figure 2.3
Schematic representation of the winding number of the SSH model, for the case of $\Delta_{0x} < 0$. The blue line describes the closed path made by when k_1 varies from $-\pi/2a$ to $\pi/2a$. The angle φ defined by $\tan\varphi = d_y/d_x$ completes a full circle and therefore the winding number is one.

only depends on the closed path of the external parameter [6] in parameter space. When the parameter is the crystal momentum this phase is called the "Zak phase" [10]. The Zak phase is related to the electronic transport property of an insulator [33]. For the SSH model the Berry phase is [10]

$$\begin{aligned}\gamma_{\pm} &= i\int_{-\frac{\pi}{2a}}^{\frac{\pi}{2a}} dk_1 \langle \pm, k_1 | \partial_{k_1} | \pm, k_1 \rangle = -\frac{1}{2}\int_{-\frac{\pi}{2a}}^{\frac{\pi}{2a}} dk_1 \partial_{k_1}\varphi \\ &= -\frac{1}{2}\Big[\varphi\left(\frac{\pi}{2a}\right) - \varphi\left(\frac{-\pi}{2a}\right)\Big] = -n\pi.\end{aligned}$$

Since $\pi/2a$ and $-\pi/2a$ are the same point, the single value property of the wave function implies that $\varphi\left(\frac{\pi}{2a}\right) - \varphi\left(\frac{-\pi}{2a}\right)$ must be a multiple of 2π. The multiplicity n is the winding number (the number of loops made by φ as k_1 covers the Brillouin zone.) For $\Delta_{0x} < 0$, it turns out that $n = 1$ and therefore the Berry phase is $\pi\,(\mathrm{mod}\,2\pi)$; for $\Delta_{0x} > 0$, $n = 0$ and the Berry phase is $0\,(\mathrm{mod}\,2\pi)$. This is because the minimum value of d_x is equal to $2\alpha_S\Delta_{0x}$. See Fig. (2.3) and Fig. (2.4).

In the SSH model chiral symmetry is preserved because $[H, \sigma^z]_+ = 0$ ($[\cdot,\cdot]_+$ is the anti-commutator). There is a robust electron edge state, the Jackiw-Rebbi zero mode [10]. As long as chiral symmetry is preserved, the edge mode will always be

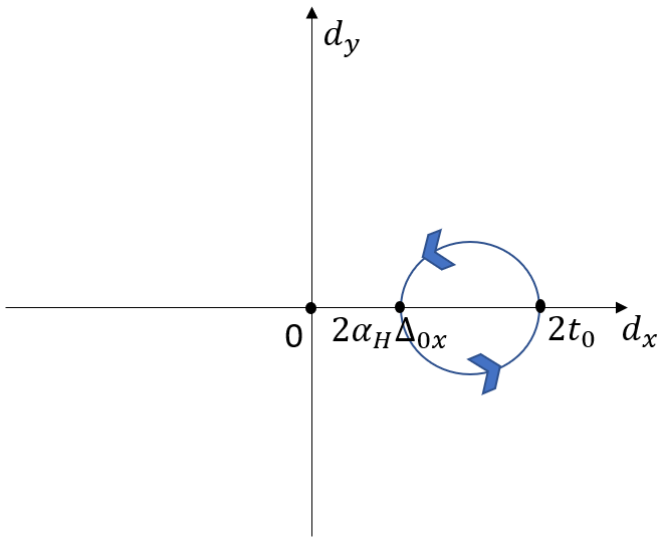

Figure 2.4
Schematic representation of the winding number of the SSH model, for the case of $\Delta_{0x} > 0$. The blue line describes the closed path made by when k_1 varies from $-\pi/2a$ to $\pi/2a$. The angle φ defined by $\tan\varphi = d_y/d_x$ does not complete a circle and therefore the winding number is zero.

present [10] in finite-size chains, provided that the winding number therein is nonzero. This is an example of symmetry-protected topological phase [30]. The physical interpretation of the existence of the edge state is that a non-trivial Zak phase is related to the non-trivial bulk polarization, so the edge state must carry charge.

2.2 The Holstein model

In its simplest realization, the Holstein model describes spinless electrons moving in one dimension with an onsite potential modulated by phonons. Its Hamiltonian is given by [18]

$$H_{\text{Holstein}} = t_0 \sum_j (c_j^\dagger c_{j+1} + H.c.) - \alpha_H \sum_j Q_j (c_j^\dagger c_j) + \frac{1}{2} m_H \sum_j \left[\dot{Q}_j{}^2 + \omega_H^2 Q_j^2 \right], \quad (2.10)$$

where Q_j is the lattice displacement at site j and α_H is the Holstein electron-phonon coupling constant. We work in a gauge where t_0 is real. At half filling, the system undergoes a Peierls instability towards a gapped site-density wave [18]. In mean field approximation, the density wave is defined by $Q_j = \frac{(-1)^j}{2}\Delta_{0z}$, where Δ_{0z} is a static order

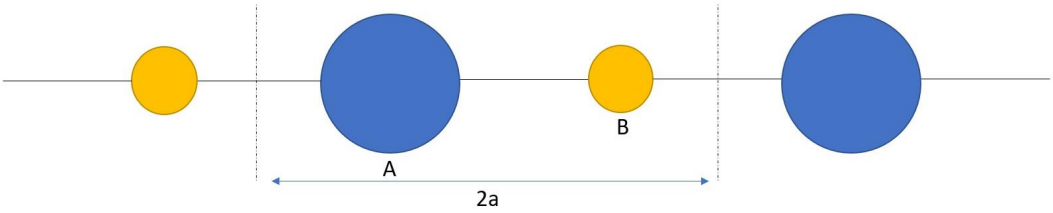

Figure 2.5
Schematic representation of the mean-field ground state of the Holstein model. The site potential is modulated between weak and strong values (single and double lines, respectively). As a result the system has a two-atom unit cell. The two sites in the unit cell are denoted as A and B sites (in blue and yellow, respectively).

parameter. It follows that the onsite potential becomes dimerized, so

$$H_{\text{Holstein,MF}} = t_0 \sum_j (c_j^\dagger c_{j+1} + h.c.) - \frac{1}{2}\alpha_H \Delta_{0z} \sum_j (-1)^j (c_j^\dagger c_j - c_{j+1}^+ c_{j+1}) + \frac{1}{2} m_H \omega_H^2 \sum_j \Delta_{0z}^2. \tag{2.11}$$

A geometric presentation of the Holstein model is given in Fig. (2.5). In the pseudospin representation, the site density wave can also be mapped onto an antiferromagnetic state by the same operators as in Eq. (2.3). Then, $\langle S_{j+1}^z \rangle \propto (-1)^{j+1} \alpha_H \Delta_{0z}/2$, and Δ_{0z} can be understood as a Néel order along z.

In Fourier space the Hamiltonian can be written as

$$H_{\text{Holstein,MF}} \approx \sum_{k_1} \begin{bmatrix} C_{k_1 A}^\dagger & C_{k_1 B}^\dagger \end{bmatrix} \mathbf{d} \cdot \boldsymbol{\sigma} \begin{bmatrix} C_{k_1 A} \\ C_{k_1 B} \end{bmatrix} + \frac{N}{2} K_H \Delta_{0z}^2, \tag{2.12}$$

where

$$\begin{aligned} d_x &= t_0 + t_0 \cos(2k_1 a) \\ d_y &= -t_0 \sin(2k_1 a) \\ d_z &= \alpha_H \Delta_{0z}. \end{aligned} \tag{2.13}$$

A, B denotes sites within one unit cell and $K_H = m_H \omega_H^2$ is the phonon stiffness.The dispersion relation of the electrons is

$$\epsilon_{k_1} = \pm \sqrt{\alpha_H^2 \Delta_{0z}^2 + 2t_0^2 + 2t_0^2 \cos(2k_1 a)}, \tag{2.14}$$

and its energy spectrum is shown in Fig. (2.6). The ground state energy of the system at half-filling is

$$E[\Delta_{0z}] \approx -\sum_{q_1} \sqrt{4a^2 t_0^2 q_1^2 + \alpha_H^2 \Delta_{0z}^2} + \frac{N}{2} K_H \Delta_{0z}^2, \tag{2.15}$$

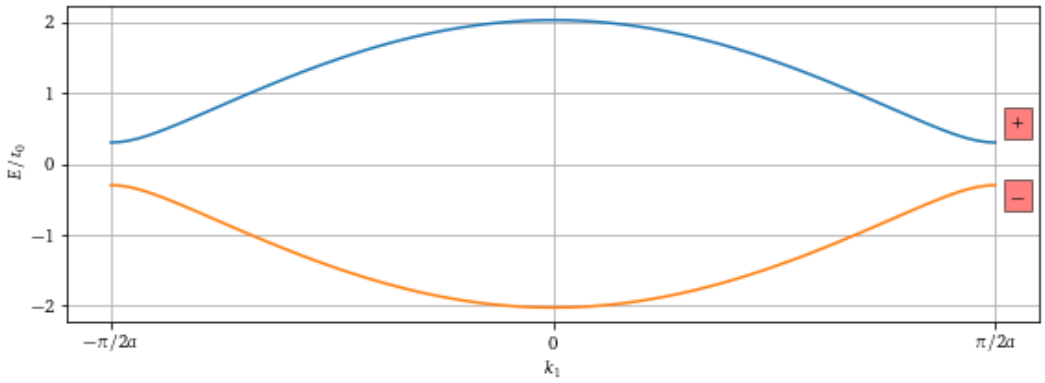

Figure 2.6
Energy spectrum of the Holstein model, where "+" means the conduction band, "-" means the valence band. We choose $a = 1$ and $\alpha_H^2 \Delta_0^2 = 0.09$.

Again the mean-field order parameter can be obtained by minimizing the energy:

$$\Delta_{0z} = \pm \frac{4at_0\Lambda}{\alpha_H} \exp -\frac{2\pi t_0 K_S}{\alpha_H^2}, \tag{2.16}$$

where Λ is a UV (ultraviolet) momentum cutoff. $\Delta_{0z} = 0$ is also a solution by minimizing the energy, however $\Delta_{0z} = 0$ always corresponds to a higher energy state in one dimension. At the mean-field level there are only two possible value of Δ_{0z} and they only differ by a sign.

The Berry phase can still be obtained from E.q (2.9), this time with $\mathbf{d}$ given by Eq. (2.13):

$$\gamma_\pm = i \int_{-\frac{\pi}{2a}}^{\frac{\pi}{2a}} dk_1 \langle \pm, k_1 | \partial_{k_1} | \pm, k_1 \rangle = -\frac{1}{2}\Big[\varphi\left(\frac{\pi}{2a}\right) - \varphi\left(\frac{-\pi}{2a}\right)\Big] - \frac{1}{2}\int_{-\frac{\pi}{2a}}^{\frac{\pi}{2a}} dk_1 \partial_{k_1} \varphi \cos\theta,$$

the Berry phase could be an arbitary value depending on the value of $\alpha_H \Delta_{0z}$. Δ_{0z} and $-\Delta_{0z}$ have the same energy, besides Δ_{0z} and $-\Delta_{0z}$ both have no well-defined Berry phase so there is no robust electron edge state since the chiral symmetry is broken.

Both the SSH state and the Holstein state of the CDW (charge density wave) break a discrete symmetry. With periodic conditions, this symmetry is $q_j \to q_{j+1}$ and $c_j \to c_{j+1}$ (translation by one lattice site). The formation of the SSH or the Holstein ground state costs elastic energy, but the gain in kinetic energy is larger, so they form stable ground state.

2.3 SSH-Holstein model

Combining Eqs. (2.1) and Eqs. (2.10), we obtain the Hamiltonian of the SSH-Holstein model:

$$H = t_0 \sum_j (c_j^\dagger c_{j+1} + h.c.) - \alpha_S \sum_j (q_j - q_{j+1})(c_j^\dagger c_{j+1} + h.c.) - \alpha_H \sum_j Q_j (c_j^\dagger c_j) + \frac{1}{2} m_S \sum_j \left[(\dot{q}_j - \dot{q}_{j+1})^2 + \omega_S^2 (q_j - q_{j+1})^2 \right] + \frac{1}{2} m_H \sum_j \left[\dot{Q}_j{}^2 + \omega_H^2 Q_j^2 \right]. \tag{2.17}$$

Based on the preceding sections, we propose the mean fields

$$q_j = \frac{(-1)^j}{2} \Delta_{0x}$$
$$Q_j = \frac{(-1)^j}{2} \Delta_{0z}. \tag{2.18}$$

Like before, the values of the mean fields can be obtained by minimizing the energy. At half filling, we can show that the energy of the system is

$$E[\Delta_{0x}, \Delta_{0z}] = -\sum_{k_1} \epsilon_{k_1} + \frac{N}{2} (K_S \Delta_{0x}^2 + K_H \Delta_{0z}^2), \tag{2.19}$$

where

$$\epsilon_{k_1} = \sqrt{2(t_0^2 + \alpha_S^2 \Delta_x^2) + 2(t_0^2 - \alpha_S^2 \Delta_{0x}^2)\cos(2k_1 a) + \alpha_H^2 \Delta_{0z}^2}. \tag{2.20}$$

Eq. (2.19) is plotted for different situations in Figs. (2.7), (2.8) and (2.9). These figures can be understood analytically by expanding k_1 in Eq. (2.20) around $\pm\pi/2a$. Then, Eq. (2.19) becomes

$$E[\Delta_{0x}, \Delta_{0z}] \approx -\sum_{q_1} \sqrt{4a^2 t_0^2 q_1^2 + 4\alpha_S^2 \Delta_{0x}^2 + \alpha_H^2 \Delta_{0z}^2} + \frac{N}{2} (K_S \Delta_{0x}^2 + K_H \Delta_{0z}^2). \tag{2.21}$$

Therefore, the conditions $\partial E / \partial \Delta_{0x} = \partial E / \partial \Delta_{0z} = 0$ give

$$\left(\sum_{q_1} \frac{1}{\sqrt{4a^2 t_0^2 q_1^2 + 4\alpha_S^2 \Delta_{0x}^2 + \alpha_H^2 \Delta_{0z}^2}} - \frac{N}{2} \tilde{K}_S \right) \Delta_{0x} = 0,$$
$$\left(\sum_{q_1} \frac{1}{\sqrt{4a^2 t_0^2 q_1^2 + 4\alpha_S^2 \Delta_{0x}^2 + \alpha_H^2 \Delta_{0z}^2}} - \frac{N}{2} \tilde{K}_H \right) \Delta_{0z} = 0, \tag{2.22}$$

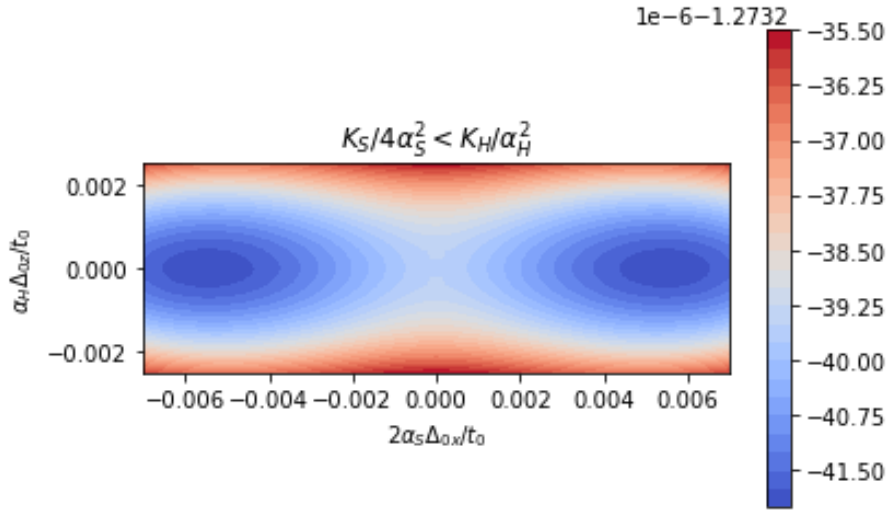

Figure 2.7
Plotting of E/t_0N for $\tilde{K}_S < \tilde{K}_H$. The mean-field order parameter minimizing the energy is $\left(\pm\frac{2at_0\Lambda}{\alpha_s}e^{-2\pi t_0\tilde{K}_S}, 0\right)$. We take $t_0\tilde{K_S} = 2$, $t_0\tilde{K_H} = 4$.

where $\tilde{K}_S = K_S/4\alpha_S^2$ and $\tilde{K}_H = K_H/\alpha_H^2$. Solving Eq. (2.22), the mean field order parameter is

$$
\begin{aligned}
(\Delta_{0x}, \Delta_{0z}) &= \left(\pm\frac{2at_0\Lambda}{\alpha_S}e^{-2\pi t_0\tilde{K}_S}, 0\right) \text{ for } \tilde{K}_S < \tilde{K}_H \\
(\Delta_{0x}, \Delta_{0z}) &= \left(0, \pm\frac{4at_0\Lambda}{\alpha_H}e^{-2\pi t_0\tilde{K}_H}\right) \text{ for } \tilde{K}_S > \tilde{K}_H \\
(\Delta_{0x}, \Delta_{0z}) &= 4at_0\Lambda e^{-2\pi t_0\tilde{K}_H}\left(\frac{1}{2\alpha_S}\sin\phi, \frac{1}{\alpha_H}\cos\phi\right) \text{ for } \tilde{K}_S = \tilde{K}_H.
\end{aligned}
\tag{2.23}
$$

In the third line of Eq. (2.23), the value of ϕ can be arbitrary because the ground state energy does not depend on it. In summary: (1) when $\tilde{K}_S < \tilde{K}_H$, the ground state displays SSH-like (bond density wave) order parameter; (2) when $\tilde{K}_S > \tilde{K}_H$, the ground state displays Holstein-like (site density wave) order parameter; (3) when $\tilde{K}_S = \tilde{K}_H$, there are a infinite number of sites with degenerate energy, therefore there would be a Goldstone mode know as "phason" [39].

The preceding observations are based on the mean-field approximation. It turns out that the zero-temperature phase diagram of Eq. (2.17) has been obtained in Ref. [18] using quantum Monte Carlo (see Fig. 2.10), which works well at large frequency. Depending on the value of parameters $\lambda_s \equiv \alpha_H^2/(K_H t_0)$ and $\lambda_b \equiv \alpha_S^2/(K_S t_0)$, there are three different phases: the SSH phase, the Holstein phase and the Luther-Emery metallic phase. When the values of the order parameters λ_b and λ_s increase the Luther-Emery metallic phase tends to vanish and there is a common boundary between the SSH and

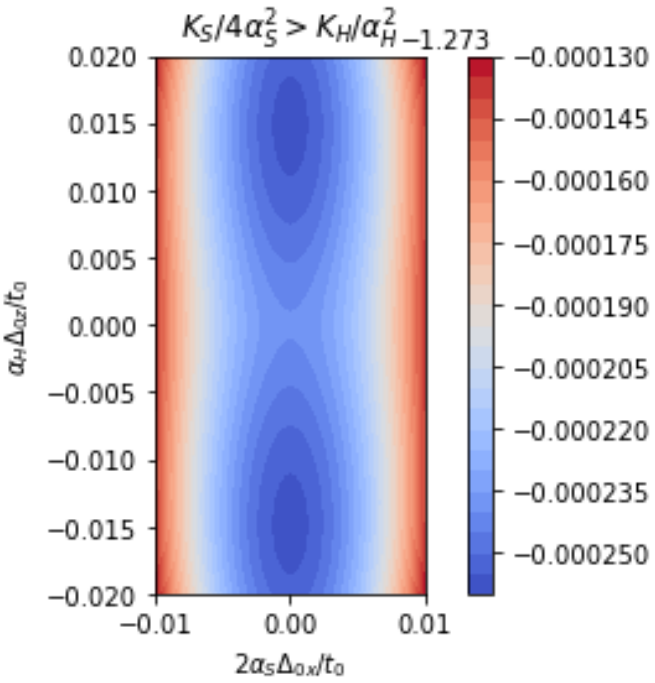

Figure 2.8
Plotting of E/t_0N for $\tilde{K}_S > \tilde{K}_H$. The mean-field order parameter minimizing the energy is $\left(0, \pm\frac{4at_0\Lambda}{\alpha_H}e^{-2\pi t_0\tilde{K}_H}\right)$. We take $t_0\tilde{K_S} = 4$, $t_0\tilde{K_H} = 2$.

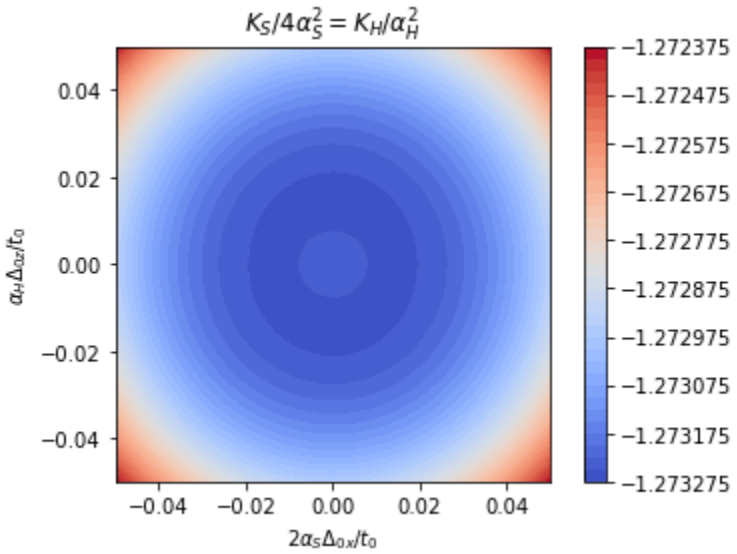

Figure 2.9
Plotting of E/t_0N for $\tilde{K}_S \approx \tilde{K}_H$. The mean-field order parameter minimizing the energy is $(\Delta_{0x}, \Delta_{0z}) = 4at_0\Lambda e^{-2\pi t_0\tilde{K}_H}\left(\frac{1}{2\alpha_S}\sin\phi, \frac{1}{\alpha_H}\cos\phi\right)$. We take $t_0\tilde{K}_S = 1.7$, $t_0\tilde{K}_H = 2$. The Goldstone mode does not appear in the case $\tilde{K}_S \approx \tilde{K}_H$ but instead appears when $\tilde{K}_S \approx \tilde{K}_H$, this is because the graph is not given by expanding k_1 around $\pm\pi/2a$, but is given by direct calculation of Eq. (2.19).

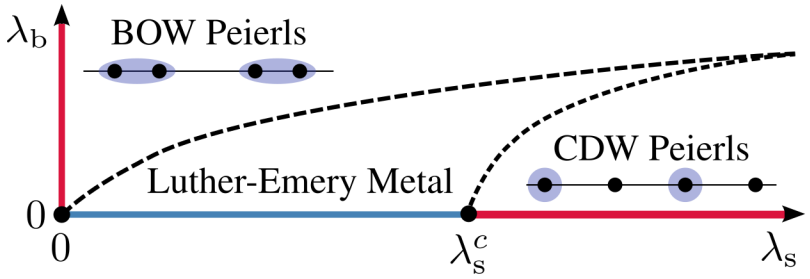

Figure 2.10
Phase diagram for SSH-Holstein model, where $\lambda_b \equiv \alpha_S^2/(K_S t_0)$, $\lambda_s \equiv \alpha_H^2/(K_H t_0)$, $K_S = m_S\omega_S^2$ and $K_H = m_H\omega_H^2$. Dashed lines are the phase boundaries. Figure taken from Ref. [18].

Holstein phases. The SSH CDW and Holstein CDW appear in the expected region. This is the region of the phase diagram where our mean-field treatment matches well the Monte Carlo prediction.

In order to realize a topological analogue of the magnetic bit, we place ourselves in the regime $\tilde{K}_S < \tilde{K}_H$. Then, we notice that Fig. (2.7) looks similar to that of a two-dimensional ferromagnet with easy-axis anisotropy. In our analogue, the two preferred (anti-parallel) orientations of the magnetization can be mapped to the order parameters Δ_{0x} and $-\Delta_{0x}$. For the case $\tilde{K}_S = \tilde{K}_H$ (see Fig (2.9)), the analouge of the magnetic anisotropy energy vanishes and the magnetization has no preferred direction. In this case, the rotational symmetry is spontaneously broken in the ground state, and the low-energy excitation is a gapless magnon; such situation is clearly not desirable for a magnetic bit.

The dynamics of the magnetization in a magnetic material is described by Landau-Lifshitz-Gilbert equation [8], which is a ground state non-linear differential equation beyond the small perturbations of the angle. Is there a similar non-perturbative equation for describing the change in the band topology? This is the main question we will address in the following chapters.

Chapter 3

Small-angle order parameter dynamics of the SSH-Holstein model

Thus far we have discussed the mean-field ground state of the SSH-Holstein model and we have described the presence of the two topologically distinct ground states therein. In this chapter, we determine the dynamics of small fluctuations around the mean-field ground state (small-angle dynamics). While insufficient to describe a topological bit, the calculations of this chapter set the notation and formalism for Chapter 4, which will concentrate on the large-angle dynamics of the order parameter.

3.1 Continuum model

We begin by introducing a continuum model, which will facilitate the calculations that follow below. The continuum model is motivated by the fact that, for half-filling, low energy excitations are concentrated in the vicinity of $k_1 = \pm\pi/2a$ [15]. This allows to write

$$\begin{aligned} c_j &= \sum_{k_1} \frac{1}{\sqrt{N}} \Psi(k_1) e^{-ik_1 x} = \sum_{k_1 \approx -k_F} \frac{1}{\sqrt{N}} \Psi(k_1) e^{-ik_1 x} + \sum_{k_1 \approx k_F} \frac{1}{\sqrt{N}} \Psi(k_1) e^{-ik_1 x} \\ &= \frac{1}{\sqrt{a}} \left(\Psi_L(x) e^{ik_F x} + \Psi_R(x) e^{-ik_F x} \right), \end{aligned} \tag{3.1}$$

and

$$\Psi_{R,L} = \sqrt{Na} \int_{-\lambda}^{\lambda} \frac{dk}{2\pi} \Psi_{k \pm K_F} e^{-ikx}, \tag{3.2}$$

where Ψ_L is the field operator for the left-moving fermions, Ψ_R is the field operator for the right-moving fermions and $k_F = \pi/2a$. Substituting Eq. (3.1) into Eq. (2.17) and

ignoring $\exp[\pm i2k_F x]$ since it is fast-varying, then the Hamiltonian of the SSH-Holstein model becomes

$$H = \int dx \Psi^\dagger h \Psi + \frac{1}{2a} m_S \int dx \Big[\dot{\Delta}_x^2 + \omega_S^2 \Delta_x^2\Big] + \frac{1}{2a} m_H \int dx \Big[\dot{\Delta}_z^2 + \omega_H^2 \Delta_z^2\Big], \tag{3.3}$$

where $\Psi = (\Psi_L, \Psi_R)$ and

$$h = -iv\sigma^z \partial_x - 2\alpha_s \Delta_x \sigma^y + \alpha_H \Delta_z \sigma^x \tag{3.4}$$

is the Hamiltonian of 1D Dirac fermions with dynamical masses and velocity $v = 2at_0$. If we define

$$\begin{aligned} -2\alpha_S \Delta_x &\equiv \Delta \sin\phi \\ \alpha_H \Delta_z &\equiv \Delta \cos\phi, \end{aligned} \tag{3.5}$$

then h is consistent with the low-energy effective Hamiltonian derived by Goldstone and Wilczek [16] for an incommensurate charge density wave (ICDW). The ICDW is a charge density wave with degenerated ground state energy, consequently, there will be a goldstone mode known as "phason", which indicates that the CDW is sliding. However, in their paper, they treat Δ and ϕ as known parameters, but in this project we want to unveil their dynamics.

3.2 Perturbations

In order to study the dynamics of the order parameter, it is important to include the effect of external perturbations. In the presence of such perturbations, Eq. (3.4) gets an additional term that we label as δH. In the low-energy subspace of R and L fermions, a generic perturbation can be written as

$$\delta H = \int dx \Psi^\dagger \delta h \Psi = \int dx \Psi^\dagger (\mathbf{B}\cdot\boldsymbol{\sigma} + B_0 \mathrm{I}) \Psi, \tag{3.6}$$

where I is the identity matrix, and $\boldsymbol{\sigma}$ is a vector of Pauli matrices in the (L,R) space. Let us discuss the physical meaning of the different components of the perturbations $(B_x, B_y, B_z) = \mathbf{B}$ and B_0. To begin with, we consider a spatial modulation of the onsite potential,

$$\delta H = \sum_j V_j c_j^\dagger c_j. \tag{3.7}$$

Using Eq. (3.1) and transferring $V(x)$ to Fourier space as $V(x) = \sum_{k_1} v_{k_1} e^{ik_1 x}$, we get

$$\begin{aligned} \delta H &\propto \int dx \Psi^\dagger [v_0 I + \Re(v_{2k_F})\sigma^x - \Im(V_{2k_F})\sigma^y]\Psi \\ &= \int dx \Psi^\dagger [v_0 I + B_x \sigma^x + B_y \sigma^y]\Psi, \end{aligned} \tag{3.8}$$

where v_0 renormalizes the chemical potential. Thus, a modulation of the onsite potential produces the perturbation B_x and B_y. If the modulation is symmetric in space ($V(x) = V(-x)$), then only B_x is present. Next, we consider the effect of a modulated strain:

$$\delta H = \sum_j V_j (c_j^\dagger c_{j+1} + H.c.), \tag{3.9}$$

which leads to

$$\delta H \propto \int dx \Psi^\dagger [2\Re(v_{2k_F})\sigma^y]\Psi = \int dx \Psi^\dagger [B_y \sigma^y]\Psi. \tag{3.10}$$

Thus a modulation of strain produces nonzero B_y. Finally, B_0 and B_z can be interpreted as scalar and vector electromagnetic potentials, respectively, because B_0 couples to the charge density and B_z enters the Hamiltonian as $(-iv\partial_x + B_z)\sigma^z$.

3.3 Effective action for the order parameters

A convenient and standard way to compute the order parameter dynamics is through the minimization of an effective action. To obtain such an effective action, we begin by writing the partition function of the system in the imaginary-time path integral formalism [3]:

$$Z = \int D(\Psi^\dagger, \Psi, \Delta_x, \Delta_z)\, e^{-S[\Psi^\dagger, \Psi, \Delta_x, \Delta_z]}, \tag{3.11}$$

where

$$S\left[\Psi^\dagger, \Psi, \Delta_x, \Delta_z\right] = \int d\tau dx \left[\Psi^\dagger \partial_\tau \Psi - \mu \Psi^\dagger \Psi\right] + \int d\tau\, (H + \delta H) \tag{3.12}$$

is the action of the system, μ is the chemical potential, and $\tau = it$ is the imaginary time. The full action in Eq. (3.12) contains both fermion and phonon (order parameter) fields. However, we are interested only in the dynamics of the order parameters.

One benefit of using the path-integral formalism is that we can integrate out the electronic degrees of freedom ($\Psi^\dagger$, Ψ) in order to quantify their influence in the dynamics of the order parameter (Δ_x, Δ_z). Because Eq. (3.12) is quadratic in the fermion fields, the integration of the electronic fields can be done exactly using the well-known formula [3]

$$\begin{aligned} \int D[\Psi^\dagger, \Psi, \Delta_x, \Delta_y] e^{-\int d\tau dx \Psi^\dagger G^{-1} \Psi} &= \int D[\Delta_x, \Delta_y] \det(G^{-1}) \\ &= \int D[\Delta_x, \Delta_y] \exp[\mathrm{Tr} \ln G^{-1}], \end{aligned} \tag{3.13}$$

where $G^{-1} = \partial_\tau - \mu + h + \delta h$, and Tr represents the trace over both space-time and the (L,R) pseudospin. In the usual jargon, G is the electronic Green's function. As a result, the partition function reads

$$Z = \int D[\Delta_x, \Delta_z] e^{-S_{\text{eff}}(\Delta_x, \Delta_z)}, \tag{3.14}$$

where $S_{\text{eff}} = S_{\text{ph}} - \text{Tr} \ln G^{-1}$ is the so-called effective action for the order parameters, and

$$S_{\text{ph}} = \int d\tau dx \left(\frac{1}{2a} m_S \left[\dot{\Delta}_x^2 + \omega_S^2 \Delta_x^2 \right] + \frac{1}{2a} m_H \left[\dot{\Delta}_z^2 + \omega_H^2 \Delta_z^2 \right] \right) \tag{3.15}$$

is the phonon-only part of the effective action. From the effective action, we obtain the dynamics of the order parameters in two steps: first, we minimize the effective action via $\delta S_{\text{eff}} / \delta \mathbf{\Delta} = 0$, and afterwards we switch back to real time. There is a problem, however. While the expression for S_{eff} is exact in principle, in practice it cannot be computed exactly because G^{-1} contains order parameter fields with arbitrary time and space dependence. As a result, we are unable to compute the trace over space and time. Thus, it is necessary to resort to approximations. The simplest approximation one can think of is to assume that the external fields are weak and that the deviations of the order parameters from their mean-field values are small. Then, one can write

$$(\Delta_x, \Delta_z) = (\Delta_{0x} + \delta\Delta_x, \Delta_{0z} + \delta\Delta_z), \tag{3.16}$$

where the first and second terms in the right hand side describe the mean-fields and the small fluctuations, respectively. As stated in Chapter 2, we choose the microscopic parameters of the Hamiltonian such that $\Delta_{0z} = 0$. Therefore, $G^{-1} = G_0^{-1} + V$, where

$$G_0^{-1} = \partial_\tau - iv\sigma^z \partial_x - \mu - 2\alpha_S \Delta_{0x} \sigma^y \tag{3.17}$$

is the mean-field part of the electronic Green function and

$$V = G^{-1} - G_0^{-1} = -2\alpha_S \delta\Delta_x \sigma^y + \alpha_H \delta\Delta_z \sigma^x + \delta h \tag{3.18}$$

is the perturbation that is assumed to be "small". Now the effective action can be written as

$$S_{\text{eff}} = S_{\text{ph}} - \text{Tr}\left[G_0^{-1} \right] + \sum_n S_n, \tag{3.19}$$

where

$$S_n = \frac{1}{n} \text{Tr}\left[(G_0 V)^n \right] \tag{3.20}$$

and we have used

$$\text{Tr}[\ln G^{-1}] = \text{Tr} \ln[G_0^{-1}] + \text{Tr} \ln(1 - G_0 V). \tag{3.21}$$

From now on we truncate the perturbative expansion of the effective action at $n = 2$. Accordingly, the angle $\phi = \arctan(-2\alpha_S \Delta_x / \alpha_H \Delta_z)$ introduced in Eq. (3.5) will be restricted to the vicinity of $\pi/2$ or $-\pi/2$, depending on the sign of Δ_{0x}. It is in this sense that the dynamics of the order parameter can be called "small-angle dynamics".

3.4 First order expansion of the action

Let us calculate the terms in the effective action that are linear in the fluctuations and in the external perturbations. We begin concentrating on $\mathrm{Tr}[G_0 V]$. Since the trace is basis-independent, we choose to write it in frequency and momentum space (ω_n, k_1). The motivation for this choice is that G_0 is diagonal in frequency and momentum space, as the mean-field ground state is static and spatially uniform. Inverting Eq. (3.17) we obtain

$$G_0(\omega_n, k_1) = \frac{i\omega_n + \mu + 2at_0 k_1 \sigma^z - 2\alpha_S \Delta_{0x}\sigma^y}{(i\omega_n + \mu)^2 - \epsilon_{k_1}^2}, \tag{3.22}$$

where

$$\epsilon_{k_1} = \sqrt{v^2 k_1^2 + 4\alpha_S^2 \Delta_{0x}^2} \tag{3.23}$$

is the excitation energy for 1D massive Dirac fermions, $\omega_n = (2n+1)\pi k_B T$ is the fermionic Matsubara frequency, T is the temperature, k_B is the Boltzmann constant,

$$V(q) = -2\alpha_S \sigma^y \delta\Delta_x(q) + \alpha_H \sigma^x \delta\Delta_z(q) + \mathbf{B}(q)\cdot\boldsymbol{\sigma} + B_0(q)\mathrm{I} \tag{3.24}$$

is the perturbation in Fourier space, and $q = (q_0, q_1) = (\omega_n - \omega_n', k_1 - k_1')$. We use the following convention for Fourier transforms:

$$\begin{aligned}\Psi(x,\tau) &= \frac{1}{\sqrt{\beta N a}} \sum_{\omega_n, k_1} \exp(-i\omega_n \tau)\exp(-ik_1 x_1)\Psi(k_1, \omega_n) \\ \Psi(\omega_n, k_1) &= \frac{1}{\sqrt{Na\beta}} \int dx d\tau \exp(i\omega_n \tau)\exp(ik_1 x)\Psi(x,\tau).\end{aligned} \tag{3.25}$$

Using these conventions, writing $k = (\omega_n, k_1)$ and defining "tr" for the trace over (L,R) pseudospin, we have

$$\begin{aligned}\mathrm{Tr}[G_0 V] &= \sum_k \mathrm{tr}\langle k|G_0 V|k\rangle = \sum_k \mathrm{tr}\, G_0(k)\langle k|V|k\rangle = \frac{1}{\sqrt{\beta N a}} \sum_k \mathrm{tr}\, G_0(k) V(0) \\ &= -\big(B_y(0) - 4\alpha_S^2 \Delta_{0x}\delta\Delta_x(0)\big) \frac{1}{\sqrt{\beta N a}} \sum_{\omega_n}\sum_{k_1} \frac{1}{(i\omega_n + \mu)^2 - \epsilon_{k_1}^2},\end{aligned} \tag{3.26}$$

where we have used the notation

$$\langle k|V|k'\rangle = \frac{1}{\sqrt{\beta N a}} V(k' - k), \tag{3.27}$$

valid because V is local in space and time. The next step is to compute the momentum and frequency sums in Eq. (3.26). We begin with the sum of Matsubara frequencies, which can be done as explained in Ref. [3]:

$$\frac{1}{\beta}\sum_{\omega_n} \frac{1}{(i\omega_n + \mu)^2 - \epsilon_{k_1}^2} = -\frac{1}{\beta}\sum_{\lambda} \mathrm{Res}\left[\frac{1}{(z+\mu)^2 - \epsilon_{k_1}^2}\right] \frac{\beta}{\exp(\beta z) + 1}\Big|_{z = z_\lambda} = \frac{f_{k_1,-} - f_{k_1,+}}{2\epsilon_{k_1}},$$

where λ is an index denoting poles, $z = i\omega_n$, "+" represents the upper electron band and "−" represents the lower electron band, as indicated in Fig. (2.2), and $f_{k_1,\pm} = 1/\left[\exp(-\beta(\pm\epsilon_{k_1} - \mu) + 1\right]$ is the Fermi-Dirac distribution function. We will be interested in the low-temperature regime, where $f_{k_1,+} \approx 0$ and $f_{k_1,-} \approx 1$. Accordingly,

$$S_1 = \left(B_y(0) - 4\alpha_S^2 \Delta_{0x} \delta\Delta_x(0)\right) \sum_{k_1} \frac{1}{2\epsilon_{k_1}} + K_S \Delta_{0x} \delta\Delta_x(0). \tag{3.28}$$

The first term of Eq. (3.28) does not contribute to the equation of motion $\delta S_{\text{eff}}/\delta\mathbf{\Delta} = 0$ because it is independent from $\delta\Delta_x$ and $\delta\Delta_z$. The second term does not contribute either because time average of the fluctuation is zero.

3.5 Second order expansion of the action

Now we calculate the terms in the effective action which are quadratic in the perturbation V. We will use the well-known formula

$$\text{Tr}[G_0 V G_0 V] = \frac{1}{\beta N a} \sum_{q_1,q_0} \frac{1}{Na} \sum_{k_1,n,n'} |\langle k_1 n|V|k_1 + q_1 n'\rangle|^2 \frac{f_{k_1,n} - f_{k_1+q_1,n'}}{\epsilon_{k_1,n} - \epsilon_{k_1+q_1,n'} + iq_0}, \tag{3.29}$$

where $n = \pm$ and $n' = \pm$ are the mean-field electronic band indices, $\epsilon_{k_1\pm} = \pm\epsilon_{k_1}$ is the band energy, $|k_1, +\rangle = (\cos(\theta_{k_1}/2), \sin(\theta_{k_1}/2))^T$ and $|k_1, -\rangle = (-\sin(\theta_{k_1}/2), \cos(\theta_{k_1}/2))^T$ are the band eigenstates, and $\cos\theta_{k_1} = 2vk_1/\epsilon_{k_1}$. At zero temperature, only $n = -n'$ contribute to Eq. (3.29). Therefore the only matrix elements to compute are

$$\begin{aligned}|\langle k_1, +|V|k_1', -\rangle|^2 = {} & 4\alpha_S^2 \cos^2\left(\frac{\theta_{k_1} + \theta_{k_1'}}{2}\right) |\delta\tilde{\Delta}_x(q)|^2 + \alpha_H^2 \cos^2\left(\frac{\theta_{k_1} - \theta_{k_1'}}{2}\right) |\delta\tilde{\Delta}_z(q)|^2 \\ & - 2i\alpha_S\alpha_H \cos\left(\frac{\theta_{k_1} + \theta_{k_1'}}{2}\right) \cos\left(\frac{\theta_{k_1} - \theta_{k_1'}}{2}\right) \left[\delta\tilde{\Delta}_x^\star(q)\delta\tilde{\Delta}_z(q) - H.c\right]\end{aligned} \tag{3.30}$$

and

$$|\langle k_1, -|V|k_1', +\rangle|^2 = |\langle k_1, +|V|k_1', -\rangle|^2_{\alpha_H \to -\alpha_H}, \tag{3.31}$$

where we have defined $\delta\tilde{\Delta}_z \equiv \delta\Delta_z + B_x/\alpha_H$ and $\delta\tilde{\Delta}_x \equiv \delta\Delta_x - B_y/2\alpha_S$. In Eq. (3.30), we have omitted the gauge fields B_0 and B_z for simplicity. We will treat them in the next chapter.

Using Eq. (3.29) we get

$$S_2 + S_{\text{ph}} = \frac{1}{2\beta L} \sum_{q_0,q_1} (\delta\tilde{\Delta}_x^\star, \delta\tilde{\Delta}_z^\star) K (\delta\tilde{\Delta}_x, \delta\tilde{\Delta}_z)^T, \tag{3.32}$$

where K is a 22 matrix. In the long wavelength and the low energy approximation, i.e. $|q_0|, v|q_1| \ll |\Delta_{0x}|$, the matrix elements of K are

$$\begin{aligned}
K_{00}(q) &\approx \frac{1}{N}\frac{\partial^2 E}{\partial \Delta_x^2}\bigg|_{(\Delta_{x0},0)} + \frac{\alpha_S^2}{24\pi t_0}\frac{v^2 q_1^2 + q_0^2}{\alpha_S^2 \Delta_{0x}^2} + m_S^2 q_0^2, \\
K_{01}(q) &\approx \frac{\alpha_S \alpha_H}{16\pi^3}\frac{a q_1 q_0}{t_0^2} = -K_{10}, \\
K_{11}(q) &= \frac{1}{N}\frac{\partial^2 E}{\partial \Delta_z^2}\bigg|_{(\Delta_{x0},0)} + \frac{\alpha_H^2}{32\pi t_0}\frac{v^2 q_1^2 + q_0^2}{\alpha_S^2 \Delta_{0x}^2} + m_H^2 q_0^2.
\end{aligned} \tag{3.33}$$

In the static and uniform configuration ($q_0, q_1 = 0$), K behaves as a matrix of spring constants,

$$\begin{aligned}
K_{00}(0) &= \frac{1}{N}\frac{\partial^2 E}{\partial \Delta_x^2}\bigg|_{(\Delta_{x0},0)} \\
K_{11}(0) &= \frac{1}{N}\frac{\partial^2 E}{\partial \Delta_z^2}\bigg|_{(\Delta_{x0},0)} \\
K_{01}(0) &= -K_{10} = 0.
\end{aligned} \tag{3.34}$$

From Eq. (3.32) we obtain the equation of motion

$$\begin{bmatrix} K_{00} & K_{01} \\ K_{10} & K_{11} \end{bmatrix} \begin{bmatrix} \delta\tilde{\Delta}_x \\ \delta\tilde{\Delta}_z \end{bmatrix} = 0. \tag{3.35}$$

Considering the spatially uniform dynamics, Eq. (3.35) can be rewritten as

$$\begin{aligned}
K_{00}(0)\delta\Delta_x + \left(\frac{1}{24\pi t_0 \Delta_{0x}^2} + m_S\right)\partial_t^2 \delta\Delta_x &= K_{00}(0)\frac{B_y}{2\alpha_S} + \left(\frac{1}{24\pi t_0 \Delta_{0x}^2} + m_S\right)\frac{\partial_t^2 B_y}{2\alpha_S} \\
K_{11}(0)\delta\Delta_z + \left(\frac{\alpha_H^2}{32\pi t_0 \alpha_S^2 \Delta_{0x}^2} + m_H\right)\partial_t^2 \delta\Delta_z &= -K_{11}(0)\frac{B_y}{\alpha_H} - \left(\frac{1}{32\pi t_0 \Delta_{0x}^2} + m_H\right)\frac{\partial_t^2 B_y}{\alpha_H}.
\end{aligned} \tag{3.36}$$

These equations describe harmonic oscillations around the local minimum $(\Delta_{0x}, 0)$ with external forces. When $B_y = 0 = B_x$ the dispersion relation for the low energy fluctuations of the order parameter can be obtained by equaling the determinant of the matrix in Eq (3.35) to zero.

This concludes our discussion of small-angle order parameter dynamics. We will not discuss further aspects of small-angle dynamics (such as collective modes), since the main goal of the present chapter is to set the technical formalism for the next chapter. Next, we will go beyond small-angle order parameter dynamics by a more judicious choice of perturbation. That will allow us to realize a proof-of-principle for the topological bit.

Chapter 4

Large-angle order parameter dynamics of the SSH-Holstein model

In the previous chapter, we studied the small-angle order parameter dynamics of the SSH-Holstein model. In the SSH-Holstein model, the charge-density wave order parameter can be written as $\Delta(\sin\phi, \cos\phi, 0)$, where ϕ is the order parameter angle and Δ is the amplitude. In Chapter 3 we studied the small-angle order parameter dynamics (ϕ close to $\pi/2$ or $-\pi/2$). However, in order to describe the dynamics across a topological phase transition, we need an equation of motion for the order parameter that will be valid for an arbitrary value of ϕ ("large angle" dynamics). The purpose of the present chapter is to introduce a method that fulfills that need and enable us to provide a proof-of-principle for the topological analogue of the magnetic bit. We have since aware of similar transformation in the literature of incommensurate charge density waves (ICDW) [16, 32, 38, 24].

In Sec. 4.1 we will introduce the method of calculation. In Sec. 4.2 we will calculate the order parameter as a function of the order parameter angle, and will derive the analogue of the magnetic anisotropy energy in our system. In Sec. 4.3 we will derive the chiral anomaly using Fujikawa method. In Sec. .4 we will calculate the contribution to the action from the regular part. In Sec. 4.5 and Sec. 4.6 we will list and solve some problems during the calculations. In Sec. 4.7 we will compare our result to earlier works [16, 32, 38, 24]. In Sec. 4.8 we will discuss the physical meaning of the anomaly term. In Sec. 4.8 we will derive the equation of motion for the order parameter involving a damping term. In Sec. 4.9 we will discuss the similarity with the Josephson effect. In Sec. 4.10 we will discuss the polarization. In Sec. 4.11 we will discuss the shape of the pulse which could induce the topological phase transition.

4.1 Chiral gauge transformation

In chapter 3, we presented a method to calculated the effective action of the order parameter and the equation of motion in the presence of external perturbations. Then, we performed perturbation theory in the vicinity of the ground state. As a result, the order parameter angle ϕ was always limited to the neighborhood of $\pm\pi/2$. In this section, using the same overall method we will introduce a gauge transformation of the coordinate which will allow us to study the same system, but in the large angular fluctuation regime.

Let us begin by recalling the electronic part of the action, obtained in Chapter 3:

$$S = \int dx d\tau \Psi^\dagger [\partial_\tau - iv\sigma^z \partial_x - \Delta(x,\tau)\mathbf{\Omega}\cdot\boldsymbol{\sigma} - \mu + \mathbf{B}\cdot\boldsymbol{\sigma} + B_0 I]\Psi, \tag{4.1}$$

where $\Omega = (\cos\phi, \sin\phi, 0)$ and ϕ is defined in Eq. (3.5). Now consider a change of variables $\Psi' = R\Psi$, where $R = \exp(-i\sigma_z\phi/2)$ is a unitary operator that rotates the left-moving and right-moving fermions in the *opposite* sense by an angle $\pi/2$. Because of this twisted sense of rotation, R can be called a chiral gauge transformation. Upon this transformation, the electronic action becomes

$$\begin{aligned} S = \int dx d\tau \Psi'^\dagger \Big[&\partial_\tau - iv\sigma^z\partial_x + \Delta(x,\tau)\sigma^x - \frac{i}{2}\sigma^z\partial_\tau\phi - \frac{v}{2}\partial_x\phi \\ &- \mu + \sigma^x(\mathbf{B}\cdot\mathbf{\Omega}) - \sigma^y[(\mathbf{B}\times\mathbf{\Omega})\cdot\hat{\mathbf{z}}] + B_z\sigma^z + I_0 \Big]\Psi'. \end{aligned} \tag{4.2}$$

Here, we notice that the time and space gradients of ϕ have been separated out from ϕ itself. The later only appears only in terms that multiply with the small external perturbation $\mathbf{B}$. Thus, this opens the door of doing perturbation theory in $\partial_\tau\phi$ and $\partial_x\phi$ instead of ϕ itself.

4.2 Magnitude of the order parameter and anisotropy energy

In Eq. (4.2) there remains a difficulty in the term $\Delta\sigma^x$. Because Δ is generally space and time dependent, the calculation of the effective action for the order parameter becomes very complicated. To overcome this difficulty, we borrow an approximation method from magnetism, for temperatures below the Curie temperature, the fluctuations in the magnitude of the magnetization are neglected because they involve higher energies than the fluctuations in the angle of the magnetization. In our model, the magnetization could be mapped to the magnitude Δ of the charge density wave order parameter. Then, we assume that Δ can be minimizing the total energy of the system for each value of ϕ. This amounts to neglecting the fluctuations of Δ around its mean-field value. Ignoring the contributions of $\mathbf{B}$, the total energy of the system is given by Eq. (2.19). In the continuum approximation (cf. Chapter 3), the sum over the wave vector can be done analytically as function of Δ and ϕ (which are treated as parameters in calculation).

The price of the analytical convenience of the continuum model is the need to introduce an ultraviolet (UV) momentum cutoff Λ. Once we have obtained the energy $E[\Delta, \phi]$, we minimize it with respect to Δ. Such minimization gives

$$\Delta_{\min} = 4at_0\Lambda \exp(-2\pi t_0(\tilde{K}_S \sin^2\phi + \tilde{K}_H \cos^2\phi)). \tag{4.3}$$

We can define a parameter γ that

$$\gamma = \frac{\Delta_0^2}{2a}(\tilde{K}_S - \tilde{K}_H). \tag{4.4}$$

If $\tilde{K}_H = \tilde{K}_S$, the magnitude of order parameter is

$$\Delta_0 = 4at_0\Lambda \exp(-2\pi t_0 \tilde{K}_H), \tag{4.5}$$

we will assume that $\tilde{K}_S, \tilde{K}_H$ are close to each other, so that

$$\Delta_{min} = \xi \cos 2\phi - \xi + \Delta_0, \tag{4.6}$$

where ξ is defined as

$$\xi = \pi t_0 \Delta_0 (\tilde{K}_S - \tilde{K}_H). \tag{4.7}$$

We will treat ξ as pertubation, which represents a first order dependence on the magnitude of order parameter.

Now we find the expression of the minimum energy (ground state energy) by substituting the minimized order parameter Δ_{min} in Eq. (2.19):

$$\begin{aligned} E_{min} = \log \frac{4at_0\Lambda\Delta_{min}}{16a^2t_0^2\Lambda^2 + \Delta_{min}^2} &\approx \log \frac{\Delta_{min}}{4at_0\Lambda} \\ &= \log(e^{-2\pi t_0(\tilde{K}_s \sin^2\phi + \tilde{K}_H \cos^2\phi)}) \\ &= -2\pi t_0 \left[\left(\tilde{K}_S - \tilde{K}_H\right) \sin^2\phi + \tilde{K}_H \right], \end{aligned} \tag{4.8}$$

thus

$$E_{min}[\phi] \approx -\frac{N\Delta_{min}^2(\phi)}{8\pi t_0}, \tag{4.9}$$

and

$$\frac{\partial E_{min}}{\partial \phi} = 0 \rightarrow \gamma \sin 2\phi = 0, \tag{4.10}$$

For $\gamma < 0$, the energy of the system reaches a local minimum at $\phi = \frac{\pi}{2}(2n+1)$, and reaches a local maximum at $\phi = n\pi$, where n is an integer.

4.3 The chiral anomaly

In section 4.1, we have seen how the electronic action changes under a chiral gauge transformation. This is not the whole story. In 1979, Kazuo Fujikawa [13, 14] pointed out that, when a chiral gauge transformation is applied to Dirac fermions in even space-time dimensions, the measure of the path integral changes as well. This change in the measure results in an additional term in the effective action, which is known as the chiral anomaly contribution. In this section, we calculate the anomaly contribution appearing in our model. We denote the anomaly part of the action as S_a.

Including the electromagnetic vector potential $A = (A_0, A_1)$, the electronic part of the action of the system can be written as [35]

$$S = -i \int d\tau dx \bar{\Psi} \left[i\tilde{\not{D}} + iM(\phi) \right] \Psi, \tag{4.11}$$

where

$$\bar{\Psi} = \Psi^\dagger \sigma^x. \tag{4.12}$$

The Hermitian and gauge-invariant derivative operator $i\tilde{\not{D}}$ is

$$i\tilde{\not{D}} = i\not{\partial} + e\tilde{\not{A}}, \tag{4.13}$$

where $\tilde{\not{A}} = \tilde{A}_\mu \gamma^\mu$ is the "Feynman slashed notation", γ^μ are Dirac gamma matrices with $\mu = 0, 1$ ($\gamma^0 = \sigma^x, \gamma^1 = -\sigma^y$), which satisfy the anti-commutation relation $[\gamma^u, \gamma^v]_+ = 2\delta^{\mu\nu}$ (we take the Fermi velocity $v = 1$), and $\tilde{A}_0 = A_0 - i\frac{v}{2e}\partial_x \phi$ and $\tilde{A}_1 = A_1 + \frac{i}{2e}\partial_\tau \phi$ are the generalized gauge fields [28]. The chemical potential μ can be absorbed by A_0 and B_z can be absorbed by A_1. The mass of the fermion is

$$M(\phi) = -\Delta(x)\cos\phi + B_x - \sigma^z (B_y - \Delta(x)\sin\phi), \tag{4.14}$$

The general formula for the partition function is

$$Z = \int D[\Psi, \bar{\Psi}, \phi, \Delta] e^{-S[\Psi, \bar{\Psi}, \phi, \Delta]} = \int D[\bar{\Psi}', \Psi', \phi, \Delta] \exp[-2 \ln \mathrm{Tr} J] e^{-S[\Psi', \bar{\Psi}', \phi, \Delta]}, \tag{4.15}$$

where J is the Jacobian and it involves singularity. The crucial part of the Fujikawa method is the singularity should be regularized, details calculations are in Appendix A. The action for the chiral anomaly is

$$S_a = -2 \ln \mathrm{Tr} J = \frac{i}{2\pi} \int d\tau dx \left[e\phi E_x + \frac{1}{4\pi v} (\partial_\tau \phi)^2 + \frac{v}{4\pi} (\partial_x \phi)^2 \right], \tag{4.16}$$

the action for the chiral anomaly in the real time is

$$S_a = \frac{-1}{2\pi} \int dt dx \left[e\phi E_x - \frac{1}{4\pi v} (\partial_t \phi)^2 + \frac{v}{4\pi} (\partial_x \phi)^2 \right]. \tag{4.17}$$

At first glance, one may be concerned with the fact that S_a appears to change under ϕ to $\phi+2\pi$. Yet, ϕ and $\phi+2\pi$ should be physically indistinguishable. This implies that $\exp(-S_a)$, which appears directly in the partition function, must be invariant under ϕ to $\phi+2\pi$. Fortunately, this turns out to be the case, as shown by the so-called Atiyah-Singer-Patodi index theorem [35]: ψ_n is an eigenvector of $i\tilde{\not{D}}$ and σ^z anticommutes with $i\tilde{\not{D}}$, then there are simultaneous zero modes ψ_i, ψ_j such that $i\tilde{\not{D}}\psi_i = 0$, $i\tilde{\not{D}}\psi_j = 0$ and $\sigma^z\psi_i = \psi_i$, $\sigma^z\psi_j = -\psi_j$. As a consequence

$$\begin{aligned}\det(J)^{-2} &= \exp\left[-\int d\tau dx \sum_n \left(\psi_n^\dagger \pi\sigma^z e^{-\tilde{\not{D}}^2/C^2}\psi_n\right)\right] \\ &= \exp\left[\pi(n_- - n_+)\right],\end{aligned} \tag{4.18}$$

where $n_{-,+}$ is the number of eigenvectors which has negative and positive eigenvalues, so obviously $n_- - n_+ = 0$.

With the presence of chiral symmetry, ϕ is forced to be $\frac{\pi}{2}$ or $-\frac{\pi}{2}$, and they correspond to two different topological phases. Therefore there will be robust edge states. What are the consequences of chiral anomaly on edge modes? Edge modes exist at boundary between the two regions with different topological states. Let us set this boundary at $x = 0$, separating a region with $\phi = -\pi/2$ for $x < 0$ from a region with $\phi = \pi/2$ for $x > 0$. The profile of ϕ is thus $\phi = -\frac{\pi}{2} + \pi\Theta(x)$ where Θ is the heavy step function, then

$$S_a = \frac{1}{2\pi}\int dtdx\Big(\frac{\pi}{2} - \pi\Theta(x)\Big)\frac{1}{2}e\epsilon^{uv}\tilde{F}_{uv}. \tag{4.19}$$

There is an observable effect due to the surface term, and this is the field theory description of the bulk-edge correspondence.

ϕ interacts with the electrical field E_x because CDW carries a charge, just the same as in the "sliding mode" of incommensurate CDW [25], which is an excited state [25], thus the ϕE_x term in sliding incommensurate CDW is nothing but a part of the the semiclassical equation of motion for charged particles in a conduction band. According to the band theory a valence band has no contribution to the conduction of electrons. However in our case we only consider the valence band and the ϕE_x term is still there, which contradicts to the band theory.

Firstly we consider pure SSH and pure Holstein individually. In the pure SSH case, it is possible for the system to have non-trivial Zak phase(crystal Berry phase), and non-trivial Zak phase is related to the non-trivial electrical dipole moment of the system[33], so there will be edge state which carries charge, which is known as Jackiw-Rebbi mode[10]. For the pure Holstein case there will be no edge state since the Zak phase is always zero. In the field theory language the edge state is

$$j^0 = \frac{\delta S}{\delta A^0} = -e\partial_x\phi = -\frac{1}{2}e\delta(x). \tag{4.20}$$

In our case, instead of edge state there is a current in the bulk

$$j^1 = \frac{\delta S}{\delta A^1} = \frac{1}{2} e \partial_t \phi, \tag{4.21}$$

the phase ϕ represents the position of the charge density wave, so the charge density wave is no longer rigid even in the case of commensurability. The sliding charge density wave is caused by the continuous transition from bond density wave to site density wave thus interacts with E_x. The argument here is incomplete since we have not considered the regular part yet, we will see the complete picture in later chapter.

4.4 Effective action of the phonon order parameter for the regular term

In the previous section, we derived the contribution to the effective action of the phonon order parameter, coming from the chiral gauge transformation. That contribution is non-perturbative. In this section, we integrate out electrons (like in Chapter.3) in order to obtain the remaining parts of the effective action. The starting point is the partition function:

$$Z \simeq \int D[\phi] e^{-S_a - S_{\text{ph}}} \det[G^{-1}(\tau, x)] = \int D[\phi] e^{-S_a - S_{\text{ph}}} \exp(\text{Tr} \ln[G^{-1}]), \tag{4.22}$$

where

$$\begin{aligned} G^{-1} = {} & \partial_\tau - iv\sigma^z \partial_x + \Delta_{min}\sigma^x + \sigma^x(\mathbf{B}\cdot\mathbf{\Omega}) - \sigma^y[(\mathbf{B}\times\mathbf{\Omega})\cdot z] + \sigma^z B_z - \mu + B_0 I \\ & - \frac{i}{2}\sigma^z \partial_\tau \phi - \frac{v}{2}\partial_x \phi - ev\sigma^z A_1 - ievA_0 \end{aligned} \tag{4.23}$$

is inverse Green function after the chiral gauge transformation. As mentioned in Chapter 3, we notice once again that the electromagnetic gauge field A_1 and A_0 can be absorbed into the terms containing B_z and B_0. With this in mind, from here on we only keep A_0 and B_z.

We define the unperturbed inverse electronic Green function as

$$G_0^{-1}(x,\tau) = \partial_\tau - iv\sigma^z \partial_{x_1} - \mu + \Delta_0 \sigma^x \tag{4.24}$$

and a perturbation

$$\begin{aligned} V(x,\tau) = {} & G_0^{-1} - G^{-1} \\ & = -\sigma^x(\mathbf{B}\cdot\mathbf{\Omega}) + \sigma^y[(\mathbf{B}\times\mathbf{\Omega})\cdot z] - \sigma^z B_z + \frac{i}{2}\sigma^z\partial_\tau\phi + \frac{v}{2}\partial_x\phi \\ & - \xi(\cos 2\phi - 1)\sigma^x + ievA_0, \end{aligned} \tag{4.25}$$

which represents the interaction of electrons with the order parameter fluctuation ϕ and with the external field $\mathbf{B}$. We consider the case where the magnitude of the interaction is much smaller than the energy gap $|V| \ll \Delta_0$. Specifically, the small parameters in Eq. (4.25) are $\mathbf{B}$, ξ, $\partial_x\phi$ and $\partial_t\phi$. Thus, a perturbative treatment on V does allow to explore arbitrary values of ϕ, such is the gain from the chiral gauge transformation in Sec. 4.1. To second order in V

$$\ln(G_0^{-1} - V) = \ln G_0^{-1} + \ln(1 - G_0 V) \approx \ln G_0^{-1} - G_0 V - \frac{1}{2} G_0 V G_0 V. \tag{4.26}$$

Therefore, the perturbative contribution to the order parameter effective action (not including the anomaly part) is

$$S[\phi] = \mathrm{Tr}(G_0 V) + \frac{1}{2}\mathrm{Tr}(G_0 V G_0 V) + S_{\mathrm{ph}}[\phi], \tag{4.27}$$

where we have omitted a term that is independent of ϕ and thus does not contribute to the equation of motion.

4.4.1 First order expansion of the action

Here we focus on the first order contribution of the action, which corresponds to

$$\begin{aligned}
\mathrm{Tr}[G_0 V] &= \frac{1}{\beta N a}\,\mathrm{tr}\sum_k \langle k|G_0 V|k\rangle \\
&= \frac{1}{\beta N a}\,\mathrm{tr}\sum_k \int dx d\tau \langle k|G_0 V|x\rangle\langle x|k\rangle \\
&= \frac{1}{\beta N a}\,\mathrm{tr}\Big[\sum_k G_0(k)\int dx d\tau - B_x(x)\cos\phi(x)\sigma^x + B_x\sin\phi\sigma^y - B_y\cos\phi\sigma^y \\
&\quad - B_y\sin\phi\sigma^x - \xi(\cos 2\phi - 1)\sigma^x + \frac{i}{2}\sigma^z\partial_\tau\phi + \frac{v}{2}\partial_x\phi - \sigma^z B_z + ievA_0\Big],
\end{aligned} \tag{4.28}$$

where tr[...] represents the trace over pseudo-spin indices. Since

$$G_0 = \frac{(i\omega_n - \mu + vk_1\sigma^z + \Delta_0\sigma^x)}{(i\omega_n + \mu)^2 - v^2k_1^2 - \Delta_0^2}, \tag{4.29}$$

we get

$$\mathrm{tr}[B_x G_0\cos\phi\sigma^x] = -2B_x\cos\phi\,\frac{\Delta_0}{(i\omega_n+\mu)^2 - v^2k_1^2 - \Delta_0^2}, \tag{4.30}$$

and

$$\mathrm{tr}[G_0\sigma^y] = 0, \tag{4.31}$$

$$\sum_{k_1} \mathrm{tr}[G_0 \sigma^z] = 0. \tag{4.32}$$

Since a total derivative term in the Lagrangian has no effect in the equation of motion, it follows that the terms involving $\partial_x \phi$ and $\partial_t \phi$ make no contribution to the effective action at first order. For the rest, we use the same calculational method as in Sec. 3.4 and we arrive at

$$\mathrm{Tr}(G_0 V) = \int dx d\tau \left(-\frac{\Delta_0}{a} B_x \tilde{K}_H \cos\phi - \frac{\Delta_0}{a} B_y \tilde{K}_H \sin\phi - \frac{\Delta_0}{a} \tilde{K}_H \xi (\cos 2\phi - 1) \right), \tag{4.33}$$

where we have taken the zero temperature limit. Since we are missing a "kinetic" term from the 1st order expansion(i.e., terms involving $\partial_\tau \phi$ or $\partial_x \phi$), so we need to consider the second order contribution.

4.4.2 Second order contribution to the action

Here we compute the second order contribution to the effective action of the order parameter. According to Appendix B,

$$\mathrm{Tr}\left[\frac{1}{2} G_0 V G_0 V \right] \simeq \int dx d\tau \ \frac{1}{8\pi v} (\partial_\tau \phi)^2 + \frac{i}{2\pi} e\phi(x) \partial_0 A_1, \tag{4.34}$$

where we have only kept the leading order derivatives terms. At first glance, the result is problematic. It is neither Lorentz invariant nor gauge invariant. The problem of gauge non-invariance is the most serious one. This is because Eq. (4.34) is obtained by doing the Matsubara sum first then the momentum sum. If we reverse the order between Matsubara sum and the momentum sum, we still get the same result if the momentum sum has a finite cutoff. To keep the invariance, one needs to do the momentum sum first from $-\infty$ to ∞, then do the Matsubara sum. So according to Appendix C the result is

$$\int d\tau dx \ \frac{1}{8\pi v} (\partial_\tau \phi)^2 + \frac{1}{8\pi} v (\partial_x \phi)^2 + \frac{i}{2\pi} e\phi(x) \partial_0 A_1 - \frac{i}{2\pi} ve\phi \partial_1 A_0. \tag{4.35}$$

4.4.3 The effective action

There is also a phonon-only action S_{ph} which should contribute to the total action, which is Eq. (3.15). Written in the coordinate (Δ, ϕ) we have

$$\partial_\tau \Delta_x(x,\tau) = \partial_\tau \frac{\Delta_0 \sin\phi}{2\alpha_S} = \frac{\Delta_0}{2\alpha_s} \partial_\tau \phi \cos\phi, \tag{4.36}$$

$$\partial_\tau \Delta_z(x,\tau) = -\partial_\tau \frac{\Delta_0}{\alpha_H} \cos\phi = \frac{\Delta_0}{\alpha_H} \partial_\tau \phi \sin\phi, \tag{4.37}$$

so the phonon-only action is

$$
\begin{aligned}
S_{\text{ph}}[\phi] &= \int d\tau dx \frac{1}{2a}\Delta_0^2 \cos^2\phi \left[\frac{\tilde{K}_S}{\omega_S^2}(\partial_t\phi)^2 - \tilde{K}_H\right] + \frac{1}{2a}\Delta_0^2 \sin^2\phi \left[\frac{\tilde{K}_H}{\omega_H^2}(\partial_t\phi)^2 - \tilde{K}_S\right] \\
&= \left(\gamma - \frac{2}{a}\Delta_0\xi\right)\int d\tau dx \sin^2\phi + \int d\tau dx \frac{1}{2a}\Delta_0^2\cos^2\phi \frac{\tilde{K}_S}{\omega_S^2}(\partial_t\phi)^2 \\
&+ \int d\tau dx \frac{1}{2a}\Delta_0^2 \sin^2\phi \frac{\tilde{K}_H}{\omega_H^2}(\partial_t\phi)^2. \qquad (4.38)
\end{aligned}
$$

Combining with Eq. (4.17), Eq. (4.33) and Eq. (4.35) we get the effective action in real time is

$$
\begin{aligned}
S_{\text{eff}}[\phi] = \int dx dt \Big(&-\frac{\Delta_0}{a}\tilde{K}_H B_x \cos\phi - \frac{\Delta_0}{a}\tilde{K}_H B_y \sin\phi - \frac{\gamma}{2}(\cos 2\phi - 1) \\
&+ \frac{1}{4\pi v}(\partial_t\phi)^2 - \frac{1}{4\pi}v(\partial_x\phi)^2 + \frac{1}{2a}\Delta_0^2(\partial_t\phi)^2\left[\frac{\tilde{K}_S}{\omega_S^2}\cos^2\phi + \frac{\tilde{K}_H}{\omega_H^2}\sin^2\phi\right] \\
&- \frac{1}{\pi}e\phi E_x\Big). \qquad (4.39)
\end{aligned}
$$

4.5 Problems

We identified three problems when we are trying to reproduce the fractional charge of the edge state. In this section, we list all the three problems.

4.5.1 Problem of non-gauge invariance

After we reverse the order between Matsubara sum and momentum sum, we seem to get a lorentz invariant term and gauge invariant term. However, in $\text{Tr}[G_0 V G_0 V]$ there is another non-gauge invariant term involving $e^2v^2|\boldsymbol{A}|^2$, for which We ignored it the calculation of Eq. (466) because we assumed the linear response. However, if we keep this term, then the $\text{Tr}[G_0 V G_0 V]$ is non-gauge invariant. This is why the authors of [32] used a regularzation.

4.5.2 Problem of non-commutation of ω_n and k_1

As mentioned in the previsous section, $\sum_{\omega_n}$ and $\int dk_1$ does not commute in the sense that if we do the sum over frequencies first we get Eq. (4.34). However if we do the integral first we get Eq. (4.35). Why don't the two operations commute?

4.5.3 Problem of "fractional charge"

It is well known if there are domain walls, then the edge states of the SSH model admit fractional charge [16]. However, in our total action we have $\frac{1}{\pi}e\phi E_x$ instead of $\frac{1}{2\pi}e\phi E_x$.

This is because the Jacobian gives a $\frac{1}{2\pi}e\phi E_x$ and $\mathrm{Tr}[\frac{1}{2}G_0VG_0V]$ gives another $\frac{1}{2\pi}e\phi E_x$. Combining the two gives an integer charge for the edge mode and hence breaks the symmetry, which is certainly not the case. So why does this happen?

4.6 Solution to the problems

All of these three problems indicate that $\mathrm{Tr}[G_0VG_0V]$ needs to be regularized. The integral (see Appendix C)

$$\int_0^\infty dk_0dk_1\frac{(-k_0^2+v^2k_1^2+\Delta_0^2)}{(k_0^2+v^2k_1^2+\Delta_0^2)^2}=\int_0^\pi d\theta\int_0^\infty dr\frac{1}{v}r\frac{\Delta_0^2-r^2\cos 2\theta}{(r^2+\Delta_0^2)^2} \tag{4.40}$$

is ill-defined, in the sense that

$$\int_0^\infty dr\frac{r^3}{(r^2+\Delta_0^2)^2}\to\infty, \tag{4.41}$$

and

$$\int_0^\infty d\theta\cos 2\phi=0. \tag{4.42}$$

so the integral becomes a case of $0\times\infty$, which is ill-defined.

We regularize this problem by adopt the Pauli-Villars regularization, i.e, we replace

$$\frac{(-k_0^2+v^2k_1^2+\Delta_0^2)}{(k_0^2+v^2k_1^2+\Delta_0^2)^2}\to\frac{(-k_0^2+v^2k_1^2+\Delta_0^2)}{(k_0^2+v^2k_1^2+\Delta_0^2)^2}-\frac{(-k_0^2+v^2k_1^2+M^2)}{(k_0^2+v^2k_1^2+M^2)^2}, \tag{4.43}$$

where M is a large-momentum cutoff that is taken to ∞ at the end. Then Eq. (**??**) becomes

$$\int_0^\pi d\theta\int_0^\infty dr\ \frac{1}{v}r\left[\frac{\Delta_0^2}{(r^2+\Delta_0^2)^2}-\frac{M^2}{(r^2+M^2)^2}\right]=0, \tag{4.44}$$

so it turns out that $\mathrm{Tr}[G_0VG_0V]=0$. Therefore the effective action totally comes from the Jacobian and the first order contribution.

4.7 Comparing with previous works

During this work, we noticed that similar works have been done independently in the context of incommensurate charge density waves [9, 38, 32, 24, 19]. In all these papers, similar diagram calculations as our $\mathrm{Tr}[G_0VG_0V]$ and the role of chiral anomaly are discussed.

In [9] the authors claim that all the contributions to the action come from the regular $\mathrm{Tr}[G_0VG_0V]$ term and they do not consider the Jacobian term. We think their argument

is not fully correct because $\mathrm{Tr}[G_0 V G_0 V]$ has singular part and needs to be regularized. Also, their expression for $\mathrm{Tr}[G_0 V G_0 V]$ is not gauge-invariant either.

In [38] the authors use a very different regularization, that is not Lorentz invariant or gauge invariant, and they choose a finite momentum cut-off which does not preserve Lorentz invariance. Actually their treatment is half relativistic and half non-relativistic. They authors claim that part of the regular term $\mathrm{Tr}[G_0 V G_0 V]$ and part of the Jacobian term contribute to the action, and the combined term is gauge invariant. The authors get the standard answer, however their method is highly non-standard because normally the regularization should be gauge invariant.

In [24] the authors claim that $\mathrm{Tr}[G_0 V G_0 V]$ does not contribute to the action and that all the contributions are from the anomaly term. Their conclusion matches our result. However, they claim that $\mathrm{Tr}[G_0 V G_0 V]$ should be neglected because it is small compared with the anomaly term. This not true because parts of $\mathrm{Tr}[G_0 V G_0 V]$ should be of the same order as the anomaly term.

In [32, 19] the authors use different approaches from ours. The effective action is computed by different methods and they use a different regularization. Our result matches their result.

Comparing with all these papers, the main difference in our result is that (i) we are considering the commensurate charge density wave (CDW). (ii) We construct the microscopic theory of the mean-field order parameter and (iii) we include an anistropy field.

We also notice that some well-cited papers, such as [37], claim that there is no anomaly contribution for massive fermions since the axial current is always conserved. However there is no contradiction with our result, because by "anomaly contribution" we mean the Jacobian contribution and the axial current is indeed conserved. However, even the axial current is conserved the Jacobian term can still lead to observable effect. The axial current conservation is

$$\langle \partial_\mu j_5^\mu \rangle = 2\langle M \bar{\Psi} \sigma^z \Psi \rangle + \frac{e}{2\pi} \epsilon_{\mu\nu} \langle \tilde{F}_{\mu\nu} \rangle, \tag{4.45}$$

where j_5 is the axial current and M is the fermion mass. When the fermion mass is non-zero, then the axial current should be conserved such that $\langle \partial_\mu j_5^\mu \rangle = 0$, this is because due to the presence of the mass gap, there is no net left mover nor right mover been created by the external electric field. Such argument agrees with the semiclassical electron dynamics in band theory [4]. Consequently, the Jacobian terms would still contribute to the action (second term on the right-hand side of Eq. (4.45)) because it needs to be there to cancel the mass contribution. We noticed a similar result has been obtained in [34] independently.

4.8 Equation of motion of the phonon order parameter

In this section we derive the equation of motion for the phonon order parameter,which is a topological analogue of the Landau-Lifshitz-Gilbert equation. The effective action

is

$$S_{\text{eff}}[\phi] = \text{Tr}[G_0 V] + S_a[\phi] + S_{\text{ph}}[\phi], \tag{4.46}$$

if we assume $\omega_S^2 = \omega_H^2$, so by variational principle $\delta S_{\text{eff}}[\phi] = 0$ the equation of motion is

$$(1+\eta)\partial_t^2\phi - v^2\partial_x^2\phi + 4\pi v\gamma \sin 2\phi + \eta\omega_H^2 B_x \sin\phi - \eta\omega_H^2 B_y \cos\phi + 4\pi e v E_x = 0, \tag{4.47}$$

where η is defined as $\eta = \frac{4\pi v \Delta_0^2 \tilde{K}_H}{a\omega_H^2}$. If we assume that ground state is homogeneous (position independent), then the equation of motion reduces to

$$(1+\eta)\partial_t^2\phi + 4\pi v\gamma \sin 2\phi + \eta\omega_H^2 B_x \sin\phi - \eta\omega_H^2 B_y \cos\phi + 4\pi e v E_x = 0. \tag{4.48}$$

The equation of motion describes the motion of a sliding commensurate CDW pinned by phonon anisotropy γ. It is well-known that impurities could pin the CDW [17], and we showed that the phonon anisotropy γ can also pin the CDW.

4.9 Effective action of the phonon order parameter involving damping

In order to form a qubit there should be a possibility of transition between two different states. In our model, we know that if ϕ moves from the local minimum $\phi = \frac{\pi}{2}$ to local minimum $\phi = -\frac{\pi}{2}$, then we can reverse the sign of order parameter Δ_x and induce a topological phase transition. However, if there is no energy loss, ϕ will permanently move between the two local minima, which is not good for creating a topological qubit. So in order to stabilize ϕ at one of the local minima, $\phi = \frac{\pi}{2}$ or $\phi = -\frac{\pi}{2}$, the system needs to dissipate energy, in other words, the system needs to be damped.

Damping of the system mainly comes from two main contributions: electrons and phonons. The mechanism for damping originating from electrons is the creation of electron-hole pairs from residual fluctuations of the order parameter, which eventually annihilate into phonons and thus dissipate energy. However, at zero temperature or at large energy gap, the energy gap for producing particle-hole pair is larger than for particle-hole pair to produce phonons, and this process is suppressed.

According to the pioneering works of Leggett and co-authors on the Caldeira-Leggett model and environmental effect on spin-boson systems [7], even a small fluctuation from the environment will cause energy dissipation in the system.

Let us connect the system to a dissipating environment. A dissipation action S_{env} describes the interaction between the system:

$$S_{\text{ph}}[\phi] = S_{\text{bulk}}[\phi] + S_{\text{env}}[\phi], \tag{4.49}$$

and $\delta S_{\text{ph}}[\phi] = 0$ describes the equation of motion including damping. In the Caldeira-Leggett model, the dissipation part of the action is [3]

$$S_{\text{env}}[\phi] = \int dx d\tau\ \phi(x) K(x - x', \tau - \tau')\phi(x', \tau'), \tag{4.50}$$

where

$$K(x,\tau)=\int_0^\infty d\omega\, J(\omega)D_\omega(x,\tau), \tag{4.51}$$

and D_ω is the phonon Green function, and $J(\omega)=\alpha|\omega|$ is the ohmic interaction with the environment and it breaks time reversal symmetry of the system. In terms of $\Delta_x(x)$ and $\Delta_z(x)$, the bulk part of the phonon action can be divided into two independent part

$$\begin{aligned} S_{\text{bulk}}[\Delta_x,\Delta_z]=&\frac{1}{2}m_s\int dxd\tau[(\partial_\tau\Delta_x)^2+4\alpha_S^2\omega_S^2\Delta_x^2]\\ &+\frac{1}{2}m_H\int dxd\tau[(\partial_\tau\Delta_z)^2+\alpha_H^2\omega_H^2\Delta_z^2]=S_{\text{bulk}}[\Delta_x]+S_{\text{bulk}}[\Delta_z], \end{aligned} \tag{4.52}$$

so each part can be mapped to the one particle case, just as Caldeira-Leggett model, so in the Fourier space

$$D_\omega(\omega_n)=D_{\omega,\Delta_x}(\omega_n)+D_{\omega,\Delta_z}(\omega_n), \tag{4.53}$$

where [3]

$$D_{\omega,\Delta_x}(\omega_n)=\frac{\omega_n^2}{\omega(\omega^2+\omega_n^2)}, \tag{4.54}$$

$$D_{\omega,\Delta_z}(\omega_n)=\frac{\omega_n^2}{\omega(\omega^2+\omega_n^2)}, \tag{4.55}$$

and ω is the frequency of the phonon mode in the environment which causes damping for the phonon in the bulk, ω_n is the frequency of phonon mode in the bulk. Transfering to real time we get [3]

$$S_{\text{env}}[\Delta_x,\Delta_z]=\int dxdtdt'\Gamma_S\left(\frac{\Delta_x(t,x)-\Delta_x(t',x)}{t-t'}\right)^2+\Gamma_H\left(\frac{\Delta_z(t,x)-\Delta_z(t',x)}{t-t'}\right)^2, \tag{4.56}$$

where Γ_S represents the coupling between a SSH-type phonon with the environment, and Γ_H represents the coupling between a Holstein type phonon with the environment.

4.9.1 Equation of motion of the phonon with damping term

Using the least-action principle and changing to coordinate ϕ,

$$\delta S_{\text{env}}=\frac{\delta S_{env}}{\delta\Delta_x}\frac{\delta\Delta_x}{\delta\phi}+\frac{\delta S_{env}}{\delta\Delta_z}\frac{\delta\Delta_z}{\delta\phi}, \tag{4.57}$$

and we transfer t' to Fourier space

$$\frac{\delta S_{\text{env}}}{\delta \Delta_x} = \int dxdtdt' \frac{2\big(\Delta_x(x,t)-\Delta_x(x,t')\big)}{(t-t')^2} \tag{4.58}$$

$$= \int dxdtdt' \big(\Delta_x(x,t)-\Delta_x(x,t')\big) D(t-t') \tag{4.59}$$

$$= \int dxdtd\omega [D(\omega)-D(0)]\Delta_x(\omega) e^{-i\omega t}, \tag{4.60}$$

since [36]

$$[D(\omega)-D(0)]\Delta_x(\omega) = -i\omega \frac{\operatorname{Im} D(\omega)}{\omega}\Delta_x(\omega), \tag{4.61}$$

$\Gamma_S \operatorname{Im} D(\omega)/\omega$ and $\Gamma_H \operatorname{Im} D(\omega)/\omega$ can be understood as renormalized coupling constants, and we ignore $\Gamma_H\gamma, \Gamma_s\gamma$, so

$$\delta S_{env} \approx \Gamma_S \Delta^2 \cos\phi\, \partial_t \sin\phi - \Gamma_H \Delta^2 \sin\phi\, \partial_t \cos\phi \tag{4.62}$$

where Γ_S,Γ_H on the right-hand side are the renormalized coupling constants. If we set $\omega_S = \omega_H$ and $\Gamma_S = \Gamma_H$, the equation of motion involving damping is

$$(1+\eta)\partial_t^2\phi + 4\pi\gamma \sin 2\phi + \eta\omega_H^2 B_x \sin\phi - \eta\omega_H^2 B_y \cos\phi + 4\pi e\nu E_x + \eta\Gamma_H\Delta_0^2\partial_t\phi = 0. \tag{4.63}$$

4.10 Analogue to Josephson effect

Josephson effect is a phenomenon of tunneling superconducting cooper pairs and they form a supercurrent. The phenomenon can happen when the two superconductors are close enough to each other with a barrier between them [20]. In particular, the DC Josephson effect is a phenomenon that the supercurrent flows through the barrier with zero or constant voltage applied. Experimentally the DC Josephson effect can be achieved by applying a bias current to the system.

When $B_x, B_y = 0$ the steady state equation of motion becomes

$$I = -4\pi\gamma \sin 2\phi, \tag{4.64}$$

where I is defined as $I = eE_x$. We notice that there is an analogy with the DC Josephson effect. The equation of motion for Josephson junction with damping is given by the Resistively Capacitance Shunted Junction model (RCSJ model) [26]:

$$I_{\text{bias}} = I_0 \sin 2\phi + \frac{1}{2eR}\partial_t\phi + \frac{C}{2eR}\partial_t^2\phi, \tag{4.65}$$

where I_{bias} is the bias current, ϕ is the phase difference between the two superconductors, I_0 is the critical supercurrent, $C/2eR\partial_t^2\phi$ is the displacement current and C is the

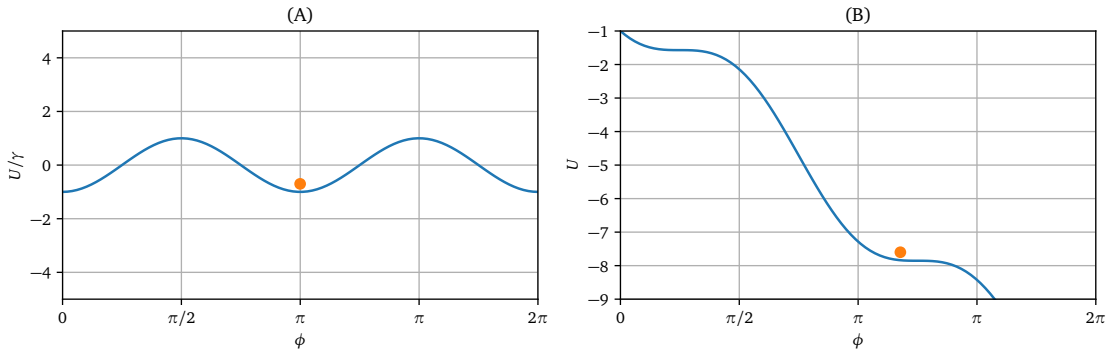

Figure 4.1
Pinning Potential for ϕ. Panel A represents the case where the charge density wave is localized, in the plot $eE_x/\gamma = 0$. Panel B represents the case where the electrical field can move the charge density wave, in the plot $eE_x/\gamma = 2$

capacitance , $1/2eR\partial_t\phi$ is the gate current and R is the resistance. This analogy has been explored in the incommensurate charge density wave system (ICDW system) [9, 17].

Back to our case, we can borrow the concept of washboard potential from the DC Josephson effect. If $|eE_x| < 4\pi\gamma$, then there will be a steady-state solution and ϕ is a constant, so in this case E_x can not induce a topological phase transition. Graphically it can be represent as Fig. (4.1). For $|E_x| > \frac{4\pi\gamma}{e}$ the potential changes to

$$U[\phi] = 2\pi\gamma\cos 2\phi - eE_x\phi, \tag{4.66}$$

so E_x can induce the topological phase transition by tilting the washboard potential. Graphically it can be represented as Fig. (4.1B). Comparing with the analogy of the Josephson effect in the ICDW system, in our case, the CDW is pinned by the phonon anisotropy γ instead of impurities, and there will also be Shapiro steps in our system, which are step-like structures in the $I-V$ diagram for the system. Shapiro steps represent it is possible to change the current without changing the voltage.

When B_x, B_y is not zero, then there will be an analogy with the fractionbe representedson effect, the energy spectrum is

$$U[\phi] = 2\pi\gamma\cos 2\phi - \sqrt{B_x^2 + B_y^2}\eta\omega_H^2\sin(\phi + \phi_0) - eE_x\phi, \tag{4.67}$$

where $\phi_0 = \arcsin\left(\frac{B_y}{\sqrt{B_x^2+B_y^2}}\right)$. So for $|eE_x| > 4\pi\gamma + \sqrt{B_x^2 + B_y^2}\eta\omega_H^2$, it is possible to induce the topological phase transition. We predict that there should be fractional Shapiro steps in our system. Fractional Shapiro steps have been used as an evidence for the appearance of Majorana fermions [11, 1], however we showed that there can be fractional Shapiro steps even without any Majorana fermions.

4.11 Polarization

The ϕ term could be understood as a polarization, and there is also a famous theorem [33] that the one dimensional electronic polarization could be calculated from the Berry phase, so using the results in Chapter2 we get the electronic polarization is

$$\begin{aligned} P &= \frac{ie}{2\pi}\oint dk_1 \,\langle -k_1|\partial_{k_1}|-,k_1\rangle \\ &= -\frac{n}{2} + \frac{1}{2\pi}\int_0^{\frac{\pi}{2a}} dk_1 \frac{a\left(\frac{t_0}{\alpha_H\Delta_z)^2} - \frac{1}{2}k_1\right)^2 + aI(k_1)}{\left[\left(\frac{t_0}{\alpha_H\Delta_z} + \frac{1}{2}k_1\right)^2 + I(k_1)\right]\sqrt{(t_0+\frac{1}{2}k_1)^2 + 1 + I(k_1)}}, \end{aligned} \tag{4.68}$$

where I is defined as

$$I(k_1) = \left(\frac{t_0}{\alpha_H\Delta_z} - \frac{1}{2}k_1\right)^2 + 2\cos(2k_1a)\left(\frac{t_0^2}{\alpha_H^2\Delta_z^2} - \frac{1}{4}k_1^2\right). \tag{4.69}$$

We notice that P is not equal to ϕ, so there seems to be a contradiction. The reason why the two results does not match still needs to be identified.

4.12 Topological phase transition induced by perturbations

In this section we will discuss the shape of perturbations (E_x, B_x, B_y) which can induce a topological phase transition.

Consider $\gamma<0$. Then without external perturbations the system will be in either one of the degenerate ground states which satisfies $\Delta_z = 0$, and which corresponds to $\phi = \frac{\pi}{2} \pmod{2\pi}$ and $\phi = \frac{3\pi}{2} \pmod{2\pi}$ respectively. The two ground state are topologically distinct, which means that for a finite chain there is a localized zero-energy electronic edge mode in one ground state, and no such mode in the other.

With an external perturbation (E_x, B_x, B_y) turned on, we are interested in what pulse shape of the perturbations can induce the topologically non-trivial phase transition. Then we will be able to construct a topological bit as an analogue of a magnetic bit.

We define the characteristic time of the anisotropy field as

$$\frac{1}{\tau_a^2} = -4\pi\nu\gamma, \tag{4.70}$$

and the characteristic times of the external fields to be

$$\begin{aligned}\frac{1}{\tau_{B_x}^2} &= 8\pi t_0 \tilde{K_H} \Delta_0^2 B_x, \\ \frac{1}{\tau_{E_x}^2} &= 4\pi v e E_x, \\ \frac{1}{\tau_{B_y}^2} &= 8\pi t_0 \tilde{K_H} \Delta_0^2 B_y,\end{aligned} \tag{4.71}$$

and the characteristic damping time to be

$$\frac{1}{\tau_d} = \eta\Gamma. \tag{4.72}$$

Moreover we will use a dimensionless time

$$\bar{t} = \frac{t}{\tau_a}, \tag{4.73}$$

which amounts to setting $1/\tau_a$ as the unit of time. Proceeding to the appropriate changes in Eq. (4.48), we find

$$(1+\eta)\partial_{\bar{t}}^2\phi - \sin 2\phi + B_x \sin\phi - B_y \cos\phi + E_x + \Gamma\partial_{\bar{t}}\phi = 0, \tag{4.74}$$

where we define the dimensionless coefficients $B_x = \tau_a^2/\tau_{B_x}^2$, $B_y = \tau_a^2/\tau_{B_y}^2$, $E_x = \tau_a^2/\tau_{E_x}^2$ and $\Gamma = \tau_a/\tau_d$.

If one can go from $\phi = \frac{\pi}{2}$ to $\phi = \frac{\pi}{2} + (2n+1)\pi$, then there will be a topological phase transition. We call the later one a "correct" minimum, otherwise it is a "wrong" minimum. We plot three phase diagrams, in the order of weak damping, medium damping and strong damping.

First we consider $B_y = 0$, the phase diagrams are Figs. (4.2), (4.3), (4.4). We can see in all the graphs there exists a critical value of E_x which could do the topological phase transition, the critical value E_x does not depend on the scale of damping. This is consistent with the analytical calculation in the previous section. The diagrams contain many "arcs" (for example in the left lower corner of Fig. 4.2), which are caused by the inertia of CDW. Even when the pulse stops, the CDW will continue to move and is finally stopped by damping. When the regions of topological phase transition increase the perturbation B_x becomes stronger, this is because $\cos 2\phi$ and $\cos\phi$ have different spectrum. The distance between the two local minimum which could lead to topological phase transition for $\cos 2\phi$ is $\pi/2$, but the distance for $\cos\phi$ is π, thus for $\cos\phi$ it is less likely to go to the wrong minimum thus increase the region of topological phase transition. When time increases, the pattern of the phase diagrams repeat themselves, this is because the potential coupled to the CDW is more or the less "periodic". Due to the ϕE_x term in the potential, the value of the potential itself is not periodic, however

the value of ϕ which minimize the potential energy is periodic since the derivative of the potential is periodic. When E_x is large, a small increase of t_0/τ_a would change the color of the phase diagram, thus we can say that the system behaves more chaotic when E_x increases. This is because for stronger E_x it is harder to say if CDW will fall into the "correct“ minimum or the "wrong" minimum. A easy thought experiment is assume the E_x becomes infinite, then where the CDW would fall becomes undefined. When pseudo magnetic field becomes stronger, then there exists a small region of E_x where the system behaves differently from the other regions, this region either consist with large red or large blue. This is because when E_x is small and for strong pseudo magnetic field, the potential energy corresponds to the pseudo magnetic field domains the energy spectrum. The period of the potential energy corresponds to the pseudo magnetic field is as twice as the period of the potential energy of the anisotropy field, thus the CDW would more stable after falling into either the "correct" or "wrong“ minimum when t_0/τ_a increases.

.

4.13 Moving domain wall

So far we have ignored the spatial contribution $\partial_x^2\phi$, we assumed that the system is isotropic in space in the ground state and only considered dynamics. In this section we consider the spatial contribution by assuming that the system prefer static configuration which minimize the energy cost, just as the classical magnetism. In this case there will be a domain wall between the two local minimum $\phi = \pi/2$ and $\phi = -\pi/2$, and we assume only the domain wall carries the time derivative component.

Consider static configuration of the ground state energy and without external perturbations, the energy of the system is

$$E = (\partial_x\phi)^2 - \frac{2\pi\gamma}{v^2}\cos 2\phi, \tag{4.75}$$

according to our assumption we know that $\partial_x\phi = 0$ when $x \to \pm\infty$, which corresponds to the case of $\phi = \pm\frac{\pi}{2}$, so the energy of the system is $E = +2\pi\gamma/v^2$ and we get

$$\frac{\partial\phi}{\partial x} = \pm\sqrt{\frac{4\pi\gamma}{v^2}}\cos\phi. \tag{4.76}$$

Integration on both sides [8] we get a quasi-static solution

$$\phi(x,t) = 2\tan^{-1}\left(e^{Q\sqrt{\frac{\gamma 4\pi}{v^2}}(x-x_0(t))}\right), \tag{4.77}$$

where $Q = \pm$ and $x_0(t)$ is the position of the domain wall. When $\sqrt{\frac{4\pi\gamma}{v^2}}$ is small and consider x is around the location of the domain wall x_0, then the action becomes

$$S[x_0, \partial_t x_0] \propto \int dx dt \frac{1}{2\lambda}(1+\eta)(\partial_t x_0)^2 - \Big(\frac{32\pi\gamma}{\lambda} + \frac{2eE_x}{\lambda} - \frac{2\eta\omega_H^2}{\lambda}(B_x+B_y)\Big)x_0, \tag{4.78}$$

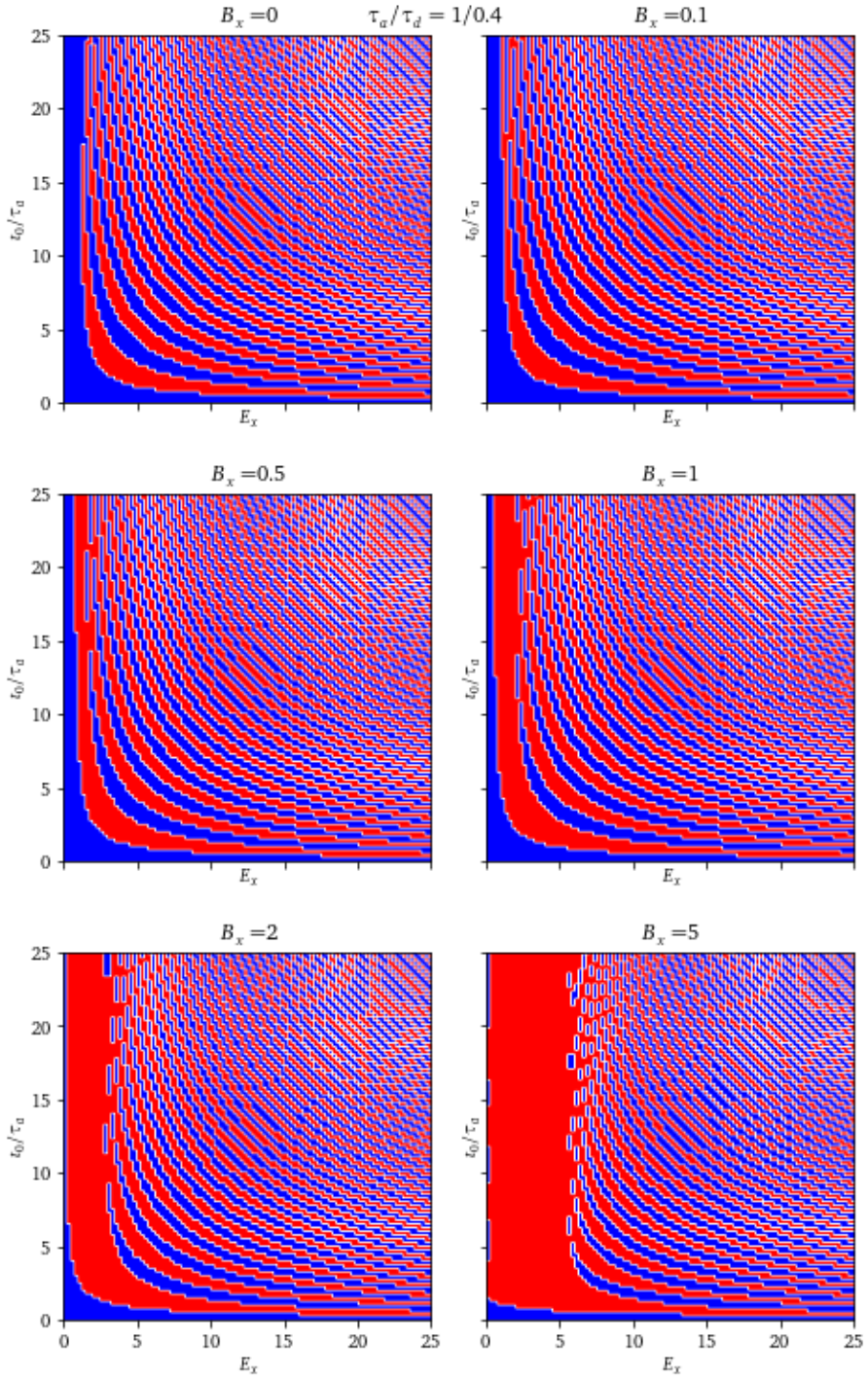

Figure 4.2
Phase diagram for weak damping. Blue: initial topology; Red: Different topology. E_x is the dimensionless electrical field, B_x is the dimensionless pseudo magnetic field in x direction. t_0/τ_a is the characteristic time for the lifetime of the plus, where we take the equation of motion to be: $\partial_{\bar{t}}^2\phi - \sin 2\phi + (B_x \sin\phi + E_x)\Theta(\frac{t_0}{\tau_a} - \bar{t}) + 0.4\partial_{\bar{t}}\phi = 0$, Θ is the Heaviside step function.

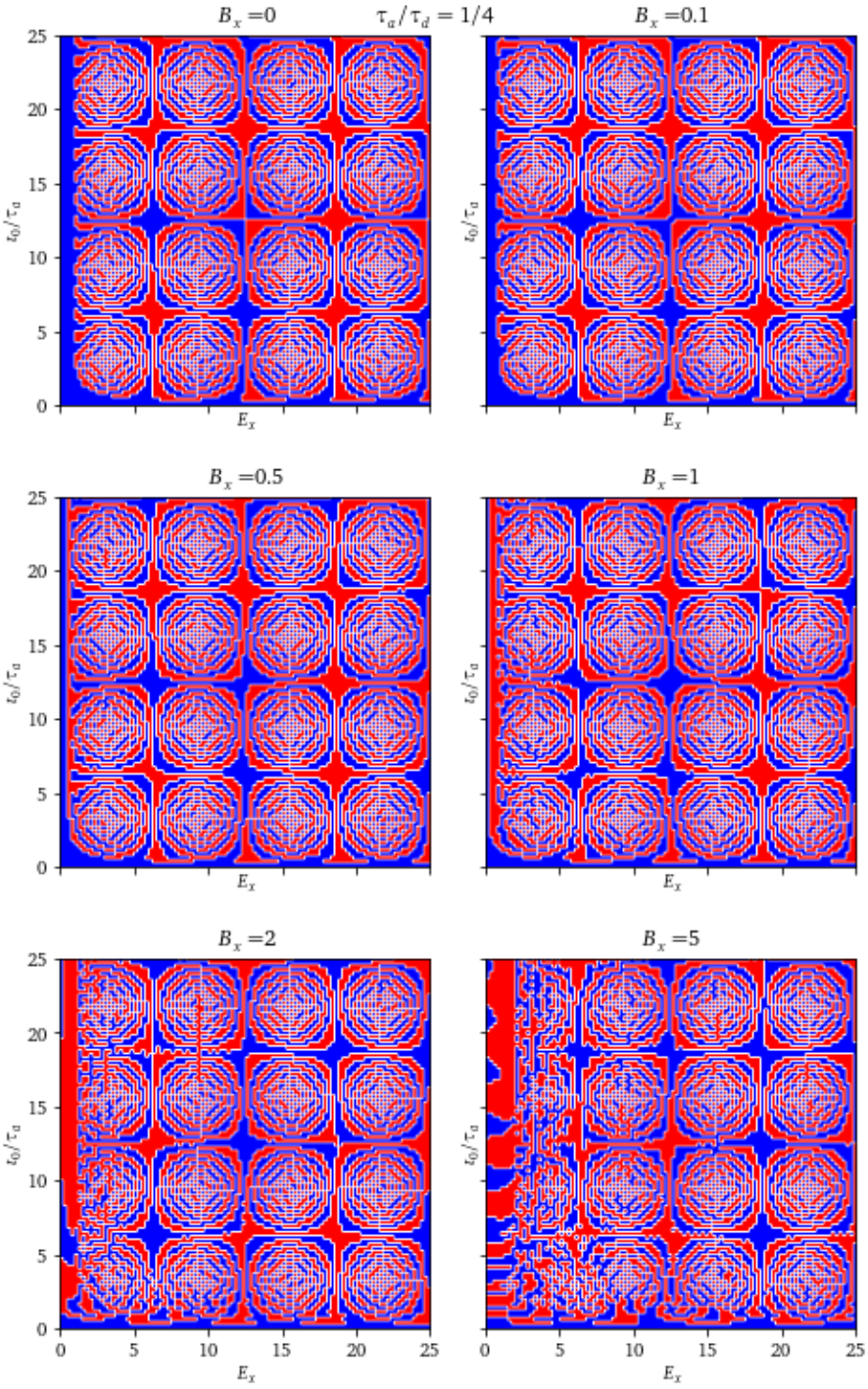

Figure 4.3
Phase diagram for medium damping. Blue: initial topology; Red: Different topology. E_x is the dimensionless electrical field, B_x is the dimensionless pseudo magnetic field in x direction. t_0/τ_a is the characteristic time for the lifetime of the plus, where we take the equation of motion to be: $\partial_{\bar{t}}^2\phi - \sin 2\phi + (B_x \sin\phi + E_x)\Theta(\frac{t_0}{\tau_a} - \bar{t}) + 4\partial_{\bar{t}}\phi = 0$, Θ is the Heaviside step function.

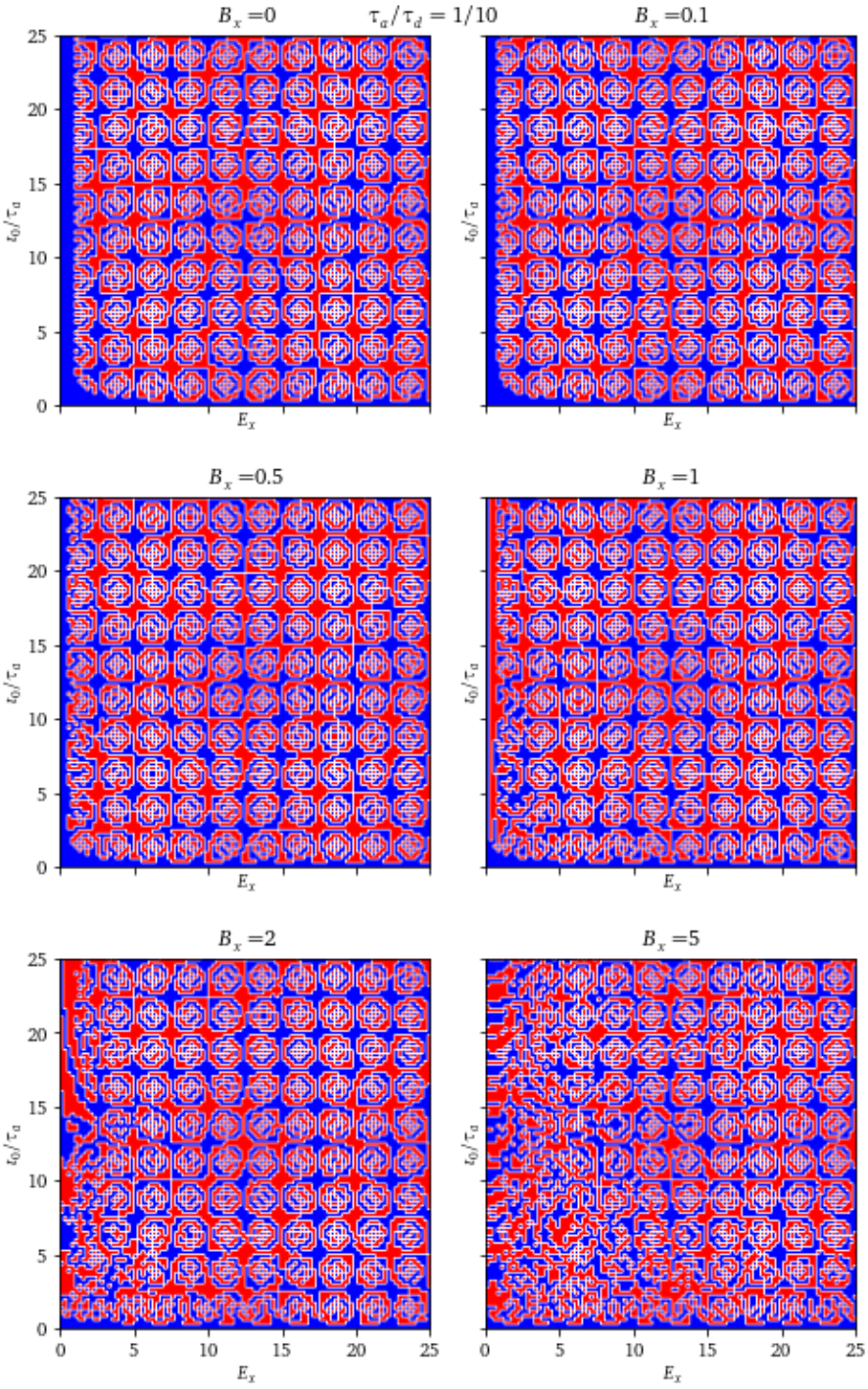

Figure 4.4
Phase diagram for strong damping. Blue: initial topology; Red: Different topology. E_x is the dimensionless electrical field, B_x is the dimensionless pseudo magnetic field in x direction. t_0/τ_a is the characteristic time for the lifetime of the plus, where we take the equation of motion to be: $\partial_{\bar{t}}^2\phi - \sin 2\phi + (B_x \sin\phi + E_x)40\Theta(\frac{t_0}{\tau_a} - \bar{t}) + 10\partial_{\bar{t}}\phi = 0$, Θ is the Heaviside step function.

where $\lambda = v^2/4\pi\gamma$, with damping the equation of motion of the domain wall is

$$\frac{1+\eta}{\lambda}\partial_t^2 x_0 + \frac{\gamma\eta}{\lambda}\partial_t x_0 + C_0 = 0, \tag{4.79}$$

where $C_0 = \frac{32\pi\gamma}{\lambda} + \frac{2eE_x}{\lambda} - \frac{2\eta\omega_H^2}{\lambda}(B_x + B_y)$. We notice that there is a solution that the velocity of the domain wall is a constant $\partial_t x_0 = v_0$, when the domain initial value that the domain wall locates at the boundary with zero velocity for $t = 0$. So even without external perturbations the domain wall can still move constantly, and in this case $v_0 = -32\pi\gamma/\Gamma\eta$. The calculation shows that there is an instability of the domain wall such that it can move inside the bulk.

Appendix A

Details calculations of the chiral anomaly term in the action

Recall the chiral gauge transformation we used in the previous section is

$$\Psi = \exp\left(-i\frac{\sigma_z\phi}{2}\right)\Psi', \tag{A.1}$$

and since $[\sigma_x, \sigma_z]_+ = 0$ we get

$$\bar{\Psi} = \bar{\Psi}'\exp\left(-i\frac{\sigma_z\phi}{2}\right), \tag{A.2}$$

after the gauge transformation the action stays the same. However, the measure should change to $D[\Psi,\bar{\Psi}] \to D[\Psi',\bar{\Psi}']\det(J)^{-2}$ since $\bar{\Psi},\Psi$ are fermionic fields. We expand the fields $\Psi,\bar{\Psi}$ in the basis of eigenfunctions of iD. $\Psi = \sum_k a_n\psi_n(x)$ and $\bar{\Psi} = \sum_n b_n\psi_n(x)$ where a_n, b_n are Grassmann numbers [14], after the gauge transformation, $\Psi' = \sum_n a'_n\psi_n(x)$ and $\bar{\Psi}' = \sum_n b'_n\psi_n(x)$, so

$$\begin{aligned} a'_n = \langle\psi_n|\Psi'\rangle &= \langle\psi_n|\exp\left(-i\frac{\sigma_z\phi}{2}\right)|\Psi\rangle \\ &= \sum_m \langle\psi_n|\exp\left(-i\frac{\sigma_z\phi}{2}\right)|\psi_m\rangle\langle\psi_m|\Psi\rangle = \sum_m J_{mn}a_m, \end{aligned} \tag{A.3}$$

where the Jacobian J is

$$J_{mn} = \frac{\delta a'_n}{\delta a_m} = \langle\psi_n|\exp\left(-i\frac{\sigma_z\phi}{2}\right)|\psi_m\rangle. \tag{A.4}$$

Fistly we assume ϕ to be infinitesimal that $\phi \to \delta\phi$. Then the Jacobian is given by

$$\begin{aligned}
\det(J)^{-2} &= \exp[-2\ln \mathrm{Tr}\, J] \\
&= \exp\Big[-2\ln\sum_n \mathrm{tr}\int d\tau dx \psi_n^\dagger(\tau,x)\exp\Big(-i\frac{\sigma_z\delta\phi}{2}\Big)\psi_n(\tau,x)\Big] \\
&\approx \exp\Big[-2\ln\sum_n \mathrm{tr}\int d\tau dx \psi_n^\dagger(\tau,x)(1-i\frac{\sigma_z\delta\phi}{2})\psi_n(\tau,x)\Big] \qquad \text{(A.5)} \\
&\approx \exp\Big[2i\sum_n \mathrm{tr}\int d\tau dx \psi^\dagger\frac{\sigma_z\delta\phi}{2}\psi_n\Big] \qquad \text{(A.6)}
\end{aligned}$$

however $\sum_n \int dx d\tau \psi_n^+(\tau,x)\psi_n(\tau,x) = \int d\tau dx \delta(0)$ is singular, thus $\det(J)^{-2}$ is ill-defined. We need to regularize this expression, which we do by adding a gauge invariant factor $-\tilde{\not{D}}^2/C^2$ where C^2 is a large momentum scale [35], so the partition function becomes

$$\begin{aligned}
\int D[\Psi,\bar\Psi,\phi]e^{-S'[\Psi,\bar\Psi,\phi]} &= \int D[\bar\Psi,\Psi,\phi]\det(J)^{-2}e^{-S[\Psi,\bar\Psi,\phi]} \\
&= \int D[\bar\Psi,\Psi,\phi]\mathrm{lim}_{C\to\infty}\exp\Big[2i\,\mathrm{tr}\int d\tau dx\frac{\delta\phi}{2}\Big(\psi_n^\dagger\sigma^z e^{-\tilde{\not{D}}^2/C^2}\psi_n\Big)\Big]e^{-S[\Psi,\bar\Psi,\phi]} \\
&= \int D[\bar\Psi,\Psi,\phi]e^{-S_a}e^{S}, \qquad \text{(A.7)}
\end{aligned}$$

the regular part action $S[\Psi,\bar\Psi,\phi] = \int d\tau dx \bar\Psi \bar G^{-1}\Psi = \int d\tau dx \Psi^+ G^{-1}\Psi$ and the anomaly part action $S_a[\Psi,\bar\Psi,\phi] = -2\,\mathrm{Tr}\Big(\psi_n^+\phi\sigma^z[1-\tilde{\not{D}}^2/C^2]\psi_n\Big)$ depends on both electrons degree of freedom (Ψ) and the phonon order parameter Δ_{min}. In order to study the dynamics of the phonon order parameter, we would like to know how the electron degrees of freedom affect the phonon order parameter. Transfer to Fourier space we get

$$\begin{aligned}
\exp\Big[2i\,\mathrm{Tr}\Big(\psi_n^\dagger\frac{\phi}{2}\sigma^z e^{-\tilde{\not{D}}^2/C^2}\psi_n\Big)\Big] &= \exp\Big[\frac{i}{4\pi^2}\int d\tau dx\,\mathrm{tr}\int dk\sigma^z e^{\frac{-k^2}{C^2}+\frac{1}{4C^2}[\gamma^\mu,\gamma^\nu]\tilde F_{\mu\nu}}\phi\Big] \\
&\approx \exp\Big[\frac{i}{16\pi^2C^2}\int d\tau dx\,\mathrm{tr}\int dk\sigma^z[\gamma^\mu,\gamma^\nu]\tilde F_{\mu\nu}\phi e^{-k^2/C^2}\Big] \\
&= \exp\Big[\int d\tau dx\frac{-i}{4\pi}\epsilon^{\mu\nu}\tilde F_{\mu\nu}\phi\Big] \\
&= \exp\Big[\frac{-i}{2\pi}\int d\tau dx e\phi E_x - \frac{1}{4\pi v}(\partial_\tau\phi)^2 - \frac{v}{4\pi}(\partial_x\phi)^2\Big], \qquad \text{(A.8)}
\end{aligned}$$

where $k=(k_0,k_1)$ and $\tilde F_{\mu\nu} = \partial_\mu\tilde A_\nu - \partial_\nu\tilde A_\mu$. The action for the chiral anomaly is

$$S_a = \frac{i}{2\pi v}\int d\tau dx\Big[e\phi E_x + \frac{1}{4\pi}(\partial_\tau\phi)^2 + \frac{v}{4\pi}(\partial_x\phi)^2\Big], \qquad \text{(A.9)}$$

the action for the chiral anomaly in the real time is

$$S_a = \frac{-1}{2\pi v}\int dtdx\Big[e\phi E_x - \frac{1}{4\pi v}(\partial_t\phi)^2 + \frac{v}{4\pi}(\partial_x\phi)^2\Big]. \qquad \text{(A.10)}$$

Appendix B

Details calculation of $\mathbf{Tr}[G_0 V G_0 V]$ (first part)

For simplicity we can write the spatial Fourier component of any function $g(x)$ as

$$\tilde{g}(k) = \frac{1}{\sqrt{\beta N a}} \int dx d\tau e^{i\omega_n \tau + i k_1 x} g(x,\tau), \tag{B.1}$$

and we define $q = (q_0, q_1)$. Since

$$\mathrm{Tr}[G_0 V G_0 V] = \frac{1}{\beta N a} \sum_{q_1,q_0} \frac{1}{Na} \sum_{k_1,n,n'} |\langle k_1 n|V(q)|k_1 + q_1 n'\rangle\langle k_1 + q_1 n'|V(-q)|k_1 n\rangle \frac{\tilde{f}_{k_1,n} - \tilde{f}_{k_1+q_1,n'}}{\epsilon_{k_1,n} - \epsilon_{k_1+q_1,n'} + iq_0}. \tag{B.2}$$

we assume the perturbations are small, so the second and higher orders of the perturbations are less important such that $\mathbf{B}^2$, and $\tilde{\gamma}^2$ are ignored. How the first order of these perturbations couple with momentum have been studied in the first order expansion except $q_0 \tilde{B_z}$, thus we can also ignored the first order contributions of the perturbations

except for $q_0\tilde{B_z}$ in the second order expansion, so

$$\begin{aligned}\mathrm{Tr}[G_0VG_0V] = \frac{1}{\beta Na}\sum_{q_1.q_0}\frac{1}{Na}\sum_{k_1}\frac{\epsilon_{k_1}+\epsilon_{k_1+q_1}-iq_0}{(\epsilon_{k_1}+\epsilon_{k_1+q_1})^2+q_0^2}\Big(\frac{1}{4}q_0^2\tilde{\phi}(q)\tilde{\phi}(q)^\star\sin^2(\frac{\theta_{k_1}+\theta_{k_1'}}{2})\\ -\frac{1}{4}q_1^2v^2\tilde{\phi}(q)\tilde{\phi}(q)^\star\sin^2(\frac{\theta_{k_1}-\theta_{k_1'}}{2})\\ +\Big(-\frac{1}{2}q_0\tilde{\phi}(q)ev\tilde{A}_1^\star(q)+\frac{1}{2}q_0\tilde{\phi}^\star(q)\tilde{A}_1(q)\Big)\sin^2(\frac{\theta_{k_1}+\theta_{k_1'}}{2})\Big)\\ +\frac{\epsilon_{k_1}+\epsilon_{k_1+q_1}+iq_0}{(\epsilon_{k_1}+\epsilon_{k_1+q_1})^2+q_0^2}\Big(\frac{1}{4}q_0^2\tilde{\phi}(q)\tilde{\phi}(q)^\star\sin^2(\frac{\theta_{k_1}+\theta_{k_1'}}{2})\\ +\frac{1}{4}q_1^2v^2\tilde{\phi}(q)\tilde{\phi}(q)^\star\sin^2(\frac{\theta_{k_1}-\theta_{k_1'}}{2})\\ +\Big(-\frac{1}{2}q_0\tilde{\phi}(q)ev\tilde{A}_1^\star(q)+\frac{1}{2}q_0\tilde{\phi}^\star(q)\tilde{A}_1(q)\Big)\sin^2(\frac{\theta_{k_1}+\theta_{k_1'}}{2})\Big),\end{aligned} \tag{B.3}$$

where we only consider linear response and potential V is treated as perturbation , so that field B_x, B_y are very small comparing with the frequency, so we consider $B_x w_n, B_x k_1 = 0$ and $B_y w_n, B_y k_1 = 0$. We also consider $B_z k_1 = 0$ but we keep $B_z\omega_n$ since it is related to the electrical field. Recall that $\epsilon_{k_1+q_1} = \sqrt{\Delta_0^2+v^2(k_1+q_1)^2}$ and $\cos\theta_{k_1+q_1} = \frac{v(k_1+q_1)}{\sqrt{\Delta^2+v^2(k_1+q_1)^2}}$ and assuming q_0, q_1 are small comparing to the energy gap. Since for any continuous function

$$F(q_0,q_1) = F(0,0)+\frac{\partial F}{\partial q_0}|_0 q_0+\frac{\partial F}{\partial q_1}|_0 q_1+\frac{1}{2}\frac{\partial^2 F}{\partial q_0^2}|_0 q_0^2+\frac{1}{2}\frac{\partial^2 F}{\partial q_1^2}|_0 q_1^2+\frac{\partial^2 F}{\partial q_0 q_1}|_0 q_0 q_1, \tag{B.4}$$

so

$$\mathrm{Tr}[G_0VG_0V] = \frac{1}{\beta Na}\sum_{q_0,q_1}\frac{1}{Na}\sum_{k_1}\frac{\sin^2\theta_{k_1}}{\epsilon_{k_1}}\left(\frac{1}{4}\tilde{\phi}^\star(0)\tilde{\phi}(0)q_0^2-\frac{1}{2}q_0\tilde{\phi}(q)ev\tilde{A}_1^\star(q)+\frac{1}{2}q_0\tilde{\phi}^\star(q)\tilde{A}_1(q)\right), \tag{B.5}$$

since

$$\frac{1}{Na}\sum_{k_1}\frac{1}{4\epsilon_{k_1}}(1-\cos^2(\theta_{k_1})) = \frac{1}{4\pi}\int_0^{\pi/2a}dk_1\frac{\Delta_0^2}{\Delta_0^2+v^2k_1^2}\frac{1}{\sqrt{\Delta_0^2+v^2k_1^2}} \approx \frac{1}{4\pi v}, \tag{B.6}$$

which value represents the smallest inverse of energy which is valid for our calculation, thus

$$\mathrm{Tr}[\frac{1}{2}G_0VG_0V] = \int dxd\tau\frac{1}{8\pi v}(\partial_\tau\phi)^2+\frac{i}{2\pi}e\phi(x)\partial_0 A_1. \tag{B.7}$$

Appendix C

Detail calculation of $\mathbf{Tr}[G_0 V G_0 V]$ (second part)

If we calculate the momentum sum first from $-\infty$ to ∞, then we calculate the Matsubara sum, the result is

$$\begin{aligned}
\mathrm{Tr}\left[\frac{1}{2}G_0 V G_0 V\right] \simeq & \int dx d\tau \ \frac{1}{8\pi v}(\partial_\tau \phi)^2 + \frac{i}{2\pi} e\phi(x)\partial_0 A_1 \\
& + \mathrm{tr}\sum_{q,k} \frac{(ik_0 + vk_1 + \Delta_0\sigma^x)}{k_0^2 + v^2 k_1^2 + \Delta_0^2} \frac{(ik_0 + vk_1 + \Delta_0\sigma^x + iq_0 + vq_1\sigma^z)}{(k_0+q_0)^2 + v^2(k_1+q_1)^2 + \Delta_0^2} \\
& \left(-\frac{1}{2}v^2 e q_1 \tilde{A}_0(q)\tilde{\phi}^\star(q) + \frac{1}{2}e v^2 q_1 \tilde{A}_0^\star(q)\tilde{\phi}(q) + \frac{1}{4}v^2 q_1^2 \tilde{\phi}(q)\tilde{\phi}^\star(q)\right) \\
& \int dx d\tau \ \frac{1}{8\pi v}(\partial_\tau \phi)^2 + \frac{i}{2\pi} e\phi(x)\partial_0 A_1 \\
& + \sum_k \frac{1}{\pi}\int_0^\infty dk_0 dk_1 \frac{(-k_0^2 + v^2 k_1^2 + \Delta_0^2)}{(k_0^2 + v^2 k_1^2 + \Delta_0^2)\left[(k_0+q_0)^2 + v^2(k_1+q_1)^2 + \Delta_0^2\right]} \\
& \left(-\frac{1}{2}v^2 e q_1 \tilde{A}_0(q)\tilde{\phi}^\star(q) + \frac{1}{2}e v^2 q_1 \tilde{A}_0^\star(q)\tilde{\phi}(q) + \frac{1}{4}v^2 q_1^2 \tilde{\phi}(q)\tilde{\phi}^\star(q)\right) \\
& = \int d\tau dx \ \frac{1}{8\pi v}(\partial_\tau \phi)^2 + \frac{1}{8\pi} v(\partial_x \phi)^2 + \frac{i}{2\pi} e\phi(x)\partial_0 A_1 - \frac{i}{2\pi} ve\phi\,\partial_1 A_0.
\end{aligned} \tag{C.1}$$

Bibliography

[1] Ramón Aguado. Majorana quasiparticles in condensed matter. *La Rivista del Nuovo Cimento*, 40(11):523–593, 2017.

[2] Amikam Aharoni et al. *Introduction to the Theory of Ferromagnetism*, volume 109. Clarendon Press, 2000.

[3] Alexander Altland and Ben D Simons. *Condensed matter field theory*. Cambridge university press, 2010.

[4] Neil W Ashcroft and N David Mermin. *Solid state physics*. Cengage Learning, 2022.

[5] B Andrei Bernevig, Taylor L Hughes, and Shou-Cheng Zhang. Quantum spin hall effect and topological phase transition in hgte quantum wells. *science*, 314(5806):1757–1761, 2006.

[6] Michael Victor Berry. Quantal phase factors accompanying adiabatic changes. *Proceedings of the Royal Society of London. A. Mathematical and Physical Sciences*, 392(1802):45–57, 1984.

[7] Amir O Caldeira and Anthony J Leggett. Path integral approach to quantum brownian motion. *Physica A: Statistical mechanics and its Applications*, 121(3):587–616, 1983.

[8] R.A. Duine. spintronic lecture notes. lecture notes Utrecht University, 2009.

[9] Ulrich Eckern and A Geier. Microscopic theory of charge-density wave systems. *Zeitschrift für Physik B Condensed Matter*, 65(1):15–27, 1986.

[10] Marcel Franz and Laurens Molenkamp. *Topological insulators*. Elsevier, 2013.

[11] SM Frolov, MJ Manfra, and JD Sau. Topological superconductivity in hybrid devices. *Nature Physics*, 16(7):718–724, 2020.

[12] Liang Fu and Charles L Kane. Topological insulators with inversion symmetry. *Physical Review B*, 76(4):045302, 2007.

[13] Kazuo Fujikawa. Path-integral measure for gauge-invariant fermion theories. *Physical Review Letters*, 42(18):1195, 1979.

[14] Kazuo Fujikawa, Kazuo Fujikawa, Hiroshi Suzuki, et al. *Path integrals and quantum anomalies*. Number 122. Oxford University Press on Demand, 2004.

[15] Thierry Giamarchi. *Quantum physics in one dimension*, volume 121. Clarendon press, 2003.

[16] Jeffrey Goldstone and Frank Wilczek. Fractional quantum numbers on solitons. *Physical Review Letters*, 47(14):986, 1981.

[17] George Grüner. The dynamics of charge-density waves. *Reviews of modern physics*, 60(4):1129, 1988.

[18] Martin Hohenadler. Interplay of site and bond electron-phonon coupling in one dimension. *Physical Review Letters*, 117(20):206404, 2016.

[19] Masakatsu Ishikawa and Hajime Takayama. On the phase dynamics of one-dimensional incommensurate charge-density-wave in an electric field. *Progress of theoretical physics*, 79(2):359–372, 1988.

[20] Brian David Josephson. Supercurrents through barriers. *Advances in Physics*, 14(56):419–451, 1965.

[21] Charles L Kane and Eugene J Mele. Quantum spin hall effect in graphene. *Physical review letters*, 95(22):226801, 2005.

[22] Charles L Kane and Eugene J Mele. Z 2 topological order and the quantum spin hall effect. *Physical review letters*, 95(14):146802, 2005.

[23] Tom Kennedy and Elliott H Lieb. Proof of the peierls instability in one dimension. In *Condensed Matter Physics and Exactly Soluble Models*, pages 85–88. Springer, 2004.

[24] IV Krive and AS Rozhavsky. Evidence for a chiral anomaly in solid state physics. *Physics Letters A*, 113(6):313–317, 1985.

[25] P Ao Lee, TM Rice, and PW Anderson. Fluctuation effects at a peierls transition. *Physical Review Letters*, 31(7):462, 1973.

[26] Konstantin K Likharev. *Dynamics of Josephson junctions and circuits*. Routledge, 2022.

[27] Xiao-Liang Qi and Shou-Cheng Zhang. Topological insulators and superconductors. *Reviews of Modern Physics*, 83(4):1057, 2011.

[28] Ralph Roskies and Fidel Schaposnik. Comment on fujikawa's analysis applied to the schwinger model. *Physical Review D*, 23(2):558, 1981.

[29] Mark S Rudner and Netanel H Lindner. Floquet topological insulators: from band structure engineering to novel non-equilibrium quantum phenomena. *arXiv preprint arXiv:1909.02008*, 2019.

[30] Todadri Senthil. Symmetry protected topological phases of quantum matter. *arXiv preprint arXiv:1405.4015*, 2014.

[31] WP Su and JR Schrieffer. Soliton dynamics in polyacetylene. *Proceedings of the National Academy of Sciences*, 77(10):5626–5629, 1980.

[32] Zhao-bin Su and B Sakita. Inhomogeneity expansion for the incommensurate charge-density-wave system. *Physical Review B*, 38(11):7421, 1988.

[33] David Vanderbilt. *Berry phases in electronic structure theory: electric polarization, orbital magnetization and topological insulators*. Cambridge University Press, 2018.

[34] Huan-Wen Wang, Bo Fu, and Shun-Qing Shen. Helical symmetry breaking and quantum anomaly in massive dirac fermions. *Physical Review B*, 104(24):L241111, 2021.

[35] Steven Weinberg. *The quantum theory of fields*, volume 2. Cambridge university press, 1995.

[36] Xiao-Gang Wen. *Quantum field theory of many-body systems: from the origin of sound to an origin of light and electrons*. OUP Oxford, 2004.

[37] Edward Witten. Fermion path integrals and topological phases. *Reviews of Modern Physics*, 88(3):035001, 2016.

[38] Victor M Yakovenko and Hsi-Sheng Goan. Influence of magnetic-field-induced spin-density-wave motion and finite temperature on the quantum hall effect in quasi-one-dimensional conductors: A quantum field theory. *Physical Review B*, 58(16):10648, 1998.

[39] Xiao-Xiao Zhang, Dirk Manske, and Naoto Nagaosa. Ultrafast excitation and topological soliton formation in incommensurate charge density wave states. *Physical Review B*, 104(12):125132, 2021.